JOC The Journal of Organic Chemistry

Article

pubs.acs.org/joc

Design and Synthesis of Labystegines, Hybrid Iminosugars from LAB and Calystegine, as Inhibitors of Intestinal α-Glucosidases: Binding Conformation and Interaction for ntSI

Atsushi Kato,*[,†] Zhao-Lan Zhang,[‡] Hong-Yao Wang,[‡] Yue-Mei Jia,[‡] Chu-Yi Yu,*[,‡] Kyoko Kinami,[†] Yuki Hirokami,[†] Yutaro Tsuji,[†] Isao Adachi,[†] Robert J. Nash,[§] George W. J. Fleet,[⊥,∥] Jun Koseki,[#] Izumi Nakagome,[#] and Shuichi Hirono*[,#]

[†]Department of Hospital Pharmacy, University of Toyama, Toyama 930-0194, Japan

[‡]Beijing National Laboratory of Molecular Science (BNLMS), CAS Key Laboratory of Molecular Recognition and Function, Institute of Chemistry, Chinese Academy of Sciences, Beijing 100190, China

[§]Institute of Biological, Environmental and Rural Sciences, Phytoquest Limited, Plas Gogerddan, Aberystwyth, Ceredigion SY23 3EB, United Kingdom

[⊥]Chemistry Research Laboratory, 12 Mansfield Road, Oxford OX1 3TA, United Kingdom

[∥]National Engineering Research Center for Carbohydrate Synthesis, Jiangxi Normal University, Nanchang 330022, PR China

[#]School of Pharmaceutical Sciences, Kitasato University, Tokyo 108-8641, Japan

Supporting Information

ABSTRACT: This paper identifies the required configuration and orientation of α-glucosidase inhibitors, miglitol, α-1-*C*-butyl-DNJ, and α-1-*C*-butyl-LAB for binding to ntSI (isomaltase). Molecular dynamics (MD) calculations suggested that the flexibility around the keyhole of ntSI is lower than that of ctSI (sucrase). Furthermore, a molecular-docking study revealed that a specific binding orientation with a CH−π interaction (Trp370 and Phe648) is a requirement for achieving a strong affinity with ntSI. On the basis of these results, a new class of nortropane-type iminosugars, labystegines, hybrid iminosugars of LAB and calystegine, have been designed and synthesized efficiently from sugar-derived cyclic nitrones with intramolecular 1,3-dipolar cycloaddition or samarium iodide catalyzed reductive coupling reaction as the key step. Biological evaluation showed that our newly designed 3(*S*)-hydroxy labystegine (**6a**) inherited the selectivity against intestinal α-glucosidases from LAB, and its inhibition potency was 10 times better than that of miglitol. Labystegine, therefore, represents a promising new class of nortropane-type iminosugar for improving postprandial hyperglycemia.

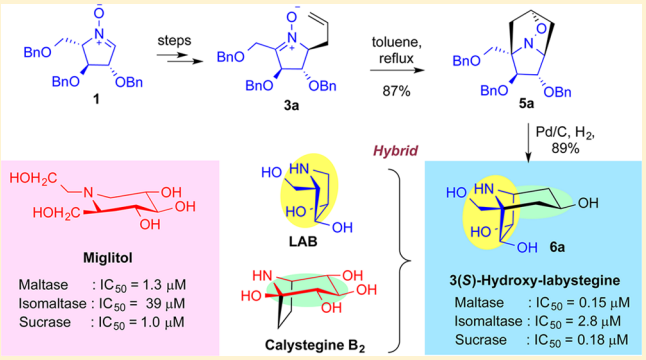

INTRODUCTION

Glycosidases are involved in several important biological processes, such as intestinal digestion, lysosomal catabolism of glycoconjugates, and post-translational modification of glycoproteins. Among these glycosidases, maltose-glucoamylase (MGAM; EC 3.2.1.20 and 3.2.1.3) and sucrase-isomaltase (SI; EC 3.2.148 and 3.2.10) are key enzymes responsible for catalyzing the last glucose-cleaving step in starch digestion. Inhibition of the α-glucosidase activity of MGAM and SI in the catabolism of dietary sugars and starches would allow potential control of blood glucose levels in individuals with type 2 diabetes. Furthermore, a recent meta-regression analysis revealed that a close relationship exists between 2 h postprandial glucose levels and cardiovascular risk below the diabetic threshold,[1] and there is growing epidemiological evidence to show that an association between postprandial hyperglycaemia and macrovascular complications exists in diabetic individuals.[2,3] Therefore, efficient α-glucosidase inhibitors have considerable potential for preventing these cardiovascular risks.

MGAM and SI, both possessing two homologous glycosyl hydrolase family 31 (GH31) catalytic subunits, are anchored to the small intestinal brush border epithelial cells: the C-terminal subunit (ctMGAM and ctSI) is near the lumen, whereas the N-terminal subunit (ntMGAM and ntSI) is near the proximal membrane-bound end.[4] ntMGAM and ctMGAM exhibit *exo* α-glucosidase activities against α-1,4-linked maltose substrates but display different specificities for malto-oligosaccharides with different lengths. In contrast, the ntSI subunit, known as

Received: February 15, 2015
Published: April 3, 2015

DOI: 10.1021/acs.joc.5b00342
J. Org. Chem. 2015, 80, 4501−4515

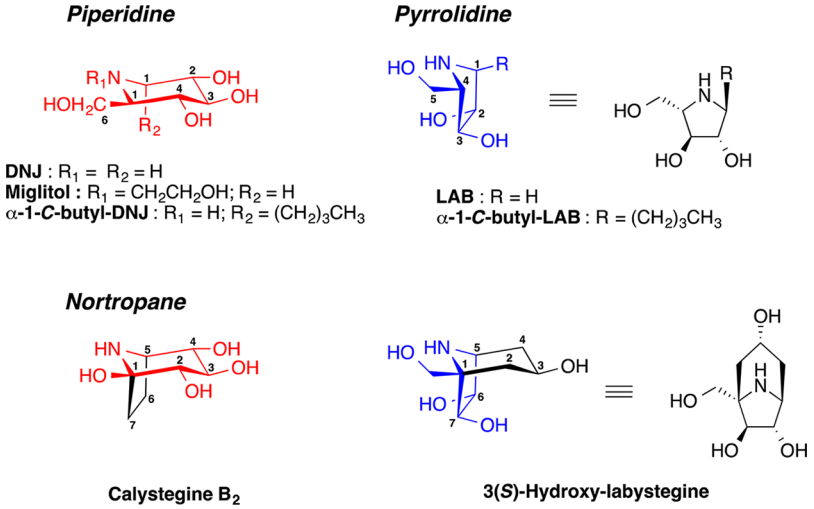

Figure 1. Chemical structures of piperidine-, pyrrolidine-, and nortropane-type iminosugars.

isomaltase, also causes hydrolysis of the α-1,6-linkages of starch and the isomaltose branch points; in addition, the ctSI subunit, classically referred to as sucrase, has glucosidase activity for the α-1,2-linkage of sucrose.[5] An ingenious synergism is proposed to exist between these enzymes in order to allow for complete digestion. These four enzymes have redundant α-1,4 activities, whereas only ntSI has high activity for α-1,6-linkages of starch and isomaltose. This difference in their activities and distribution is closely related to the component ratio of α-1,4 linkages to α-1,6-linkages in human dietary starch, which is 19:1.

The ntMGAM and ntSI are ~60% identical in amino acid sequence and higher than with the N-and C-terminal domains associated with the same enzymes (~40% sequence identity).[6−8] These sequence differences affect the inhibition specificity. In comparison with binding potential against MGAM and SI, acarbose has been shown to be an efficient inhibitor of the ctMGAM and ctSI (sucrase) but a weaker inhibitor of the ntSI (isomaltase).[9−12] These results are in agreement with previous reports on the structural of the ntMGAM−acarbose complex. Acarbose appears to bind to the ntMGAM-active site mainly through side-chain interactions with its acarvosine unit; its glycone rings have almost no interactions with amino acid residues.[8] The systematic analysis and comparison of the inhibition potencies and specificity of a range of inhibitors is needed in order to obtain a good understanding of the structural requirements for substrate reorganization and tight binding in these intestinal α-glucosidases.

Iminosugars are analogues of pyranoses and furanoses in which the ring oxygen has been replaced by nitrogen (Figure 1).[13−15] They inhibit glycosidases by mimicking the corresponding substrate or the transition-state intermediates of various glycosidases.[16] The intestinal α-glucosidase inhibitor miglitol was introduced on the market for the treatment of type 2 diabetes in 1996.[17−19] Miglitol is designed from the naturally occurring 1-deoxynojirimycin (DNJ), which closely mimics the D-glucose structure. This structural similarity to D-glucose can cause side effects such as diarrhea and impairment of liver function because it shows nonspecific α-glucosidase inhibition in various organs.[20−22] For better drugs, it is therefore useful to elucidate the structural requirements for the design of selective α-glucosidase inhibitors lacking the piperidine structures that can so closely resemble glucose. Following our recent work concerning the structure−activity relationships of pyrrolidine iminosugars,[23−26] we have recently reported the synthesis and biological evaluation of a series of α-1-*C*-alkylated 1,4-dideoxy-1,4-imino-L-arabinitol (LAB) derivatives as a new class of promising compounds that can be used to treat postprandial hyperglycemia.[27] Our results indicate that the structural similarity to D-glucose is not always necessary for recognition and tight-binding with ntMGAM. Considering these characteristic ligand−ntMGAM interactions, we turned our attention to the inhibition activities and binding interactions against ntSI and ctSI. These enzymes are essential for the processing of dietary carbohydrates in the same way as MGAM. A recent study revealed that a close relationship exists between expression of SI in colon mucosa and progression to carcinoma[28] and metastatic colon adenocarcinoma.[29] The reason for the observed up-regulation of SI in these colon cancers is not apparent yet, but it is possibly related to its metabolic activity.

The overall aim of this study was to generate iminosugars with suitable structural moieties of iminosugar inhibitors for active-site binding to SI and to provide general guidelines on the effective design of nonpiperidine-based intestinal α-glucosidase inhibitors. In the present study, we first constructed the three-dimensional structures of the rat ntSI and ctSI by performing homology modeling. Furthermore, on the basis of these protein structures, we performed molecular docking simulations to predict the docking configurations of miglitol, α-1-*C*-butyldeoxynojirimycin (α-1-*C*-butyl-DNJ), and α-1-*C*-butyl-1,4-dideoxy-1,4-imino-L-arabinitol (α-1-*C*-butyl-LAB) into ntSI (isomaltase). Using this information, a new class of nortropane-type iminosugars, labystegines, hybrid iminosugars from LAB and calystegine, were designed as a novel class of intestinal α-glucosidase inhibitors, which includes their suppressive effects on blood glucose levels using an isomaltose loading test and their binding conformations and stabilization energies with ntSI with the intention of determining the extent of differences to miglitol. Labystegines and their derivatives will be synthesized via sugar-derived cyclic nitrone chemistry developed by our research group as well as others.[30−32] Employing D-xylose-derived cyclic nitrone **1** as starting material, the nortropane scaffolds of labystegines can be constructed following the protocol of intramolecular [3 + 2] 1,3-dipolar

DOI: 10.1021/acs.joc.5b00342
J. Org. Chem. 2015, 80, 4501−4515

cycloaddition developed by Goti[30] and/or intramolecular samarium iodide catalyzed reductive coupling reaction developed by our research group.[32]

RESULTS AND DISCUSSION

Protein Structures with Homology Modeling Method. A comparison of the structures of ntSI (isomaltase) and ctSI (sucrase) will provide improved insight into their inhibitory activities on α-1,6- and α-1,2-linked substrates and should allow the design of new potent and specific inhibitors. At first, we created three-dimensional structures of the rat ntSI and ctSI with a homology modeling method, based on human isomaltase and human maltase, respectively. These predicted three-dimensional structures were relaxed by a molecular dynamics (MD) method. From these minimized structures as initial coordinates, we performed MD calculations to sample the keyhole structures. The 250 keyhole structures found were saved and clustered. Parts A and B of Figure 2 show the clustering dendrograms for the predicted rat ntSI and ctSI obtained from these results. As shown in Figure 2, we found that the number of representative structures for rat ctSI (sucrase) was larger than for rat ntSI (isomaltase) when we focused on the same criterion shown by the red dashed line. This fact suggests that the flexibility around the keyhole of sucrase is greater than that of isomaltase. Thus, to consider the difference of keyhole flexibility between isomaltase and sucrase, we have used the one and seven representative keyhole structures selected above with the same criteria in each docking calculation, respectively.

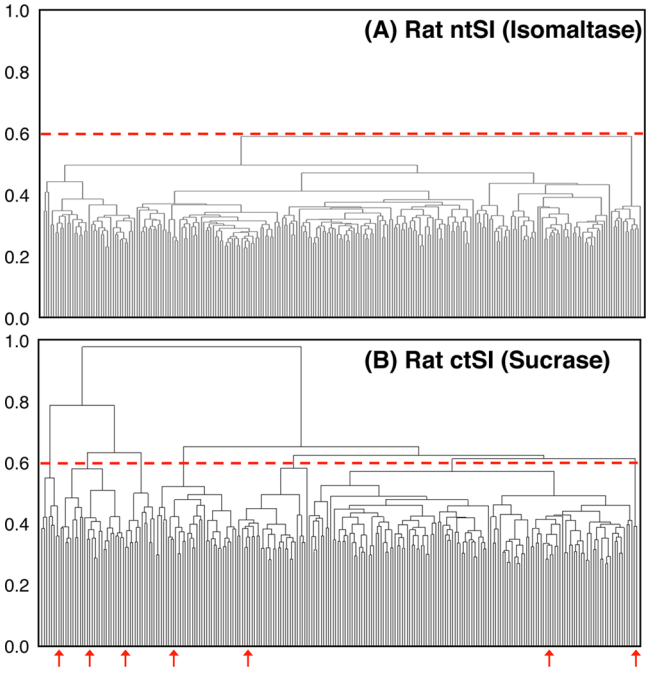

Figure 2. Clustering dendrogram for keyhole structures of predicted (A) rat ntSI and (B) ctSI obtained from each molecular dynamics simulation.

Docking Study of Miglitol, α-1-*C*-butyl-DNJ, and α-1-*C*-butyl-LAB against ntSI. To understand the structural basis of the interaction of miglitol, α-1-*C*-butyl-DNJ, and α-1-*C*-butyl-LAB with isomaltase (ntSI), we first performed molecular docking simulation of these inhibitors with one keyhole of predicted rat ntSI. Figure 3 shows the binding conformations (Figure 3A−C) and ligand/protein interactions (Figure 3D−F) for rat ntSI. Miglitol, α-1-*C*-butyl-DNJ, and α-1-*C*-butyl-LAB were observed to bind to the same hydrophobic pocket consisting of Trp370, Ile434, Trp512, Trp612, and Phe648 of rat ntSI. It is noteworthy that the binding orientation of miglitol was slightly different from that of α-1-*C*-butyl-LAB and α-1-*C*-butyl-DNJ, whereas the hydrogen bonds formed to Asp398, Trp477, Asp514, and Asp615 in ntSI were maintained in all models (Figure 3D−F). The butyl group of α-1-*C*-butyl-DNJ and α-1-*C*-butyl-LAB has a favorable interaction with the hydrophobic pocket (Ile276, Trp370, Trp477, and Phe648). The hydroxyethyl group of miglitol heads for the same hydrophobic pocket, whereas the terminal hydroxyl group gravitates toward the hydrophilic part of the active site and forms hydrogen bonds with Asp274 (Figure 3A,C). For the clarification of the difference, we next analyzed the binding stabilization energies (Δ*E*s) between each ligand and ntSI (isomaltase).

Table 1 shows that the negative logarithmic values of the half-maximal inhibitory concentration (pIC_{50}), calculated Δ*E*'s, and relative energies (ΔΔ*E*'s) of each ligand for rat ntSI (isomaltase). The binding energies (Δ*E*) for miglitol, α-1-*C*-butyl-DNJ, and α-1-*C*-butyl-LAB are −68.89, −77.11, and −75.88 (kcal/mol), respectively. These results were consistent with the experimental results (pIC_{50}) showing that α-1-*C*-butyl-DNJ has higher inhibitory activity against isomaltase than both α-1-*C*-butyl-LAB and miglitol, with pIC_{50} for each ligand of 4.41, 6.35, and 5.33 [log (μM^{-1})], respectively. For further confirmation, we also constructed the three-dimensional models of the α-1-*C*-butyl-LAB−human ntSI complex. The docking calculation was performed under the same conditions as the docking calculations of rat ntMGAM using the X-ray structures of human ntSI (PDB ID: 3LPP).

The binding energy (Δ*E*), as estimated from the three-dimensional structures of the compound with human ntSI, suggested that the α-1-*C*-butyl-LAB would be an inhibitor of human ntSI as well as that from the rat (Table 2).

From the viewpoint of binding interactions, the main difference in binding affinity could be explained by the difference in van der Waals interactions. In particular, the CH−π interaction is a very important factor for their affinity. As shown in Figure 3E,F, α-1-*C*-butyl-DNJ and α-1-*C*-butyl-LAB were found to bind to isomaltase with the same orientation. Both compounds showed hydrogen bonding (Asp514 and Asp615) and the CH−π interaction (Trp370 and Phe648). However, the six-membered ring of α-1-*C*-butyl-DNJ lies closer to Trp370 and Phe648 than the five-membered ring of α-1-*C*-butyl-LAB (Figure 4). These differences in CH−π interaction may explain the differences in potency of inhibition against isomaltase.

Influence of α-1-*C*-Alkyl Chain Length against Binding Energy in the Complex Structure. In order to clarify the depth and space of the hydrophobic pocket of ntSI (isomaltase) and to predict an acceptable alkyl chain length at the anomeric position, we prepared α-1-*C*-butyl-LAB, α-1-*C*-heptyl-LAB, and α-1-*C*-nonyl-LAB and constructed three-dimensional structures of the ntSI (isomaltase) complexed with them. Table 3 shows the negative logarithmic values of half-maximal inhibitory concentration (pIC_{50}) values, calculated binding energies (Δ*E*'s), and relative energies (ΔΔ*E*'s) of α-1-*C*-butyl-LAB, α-1-*C*-heptyl-LAB, and α-1-*C*-nonyl-LAB for rat isomaltase. The values of binding energies (Δ*E*'s) for each ligand are −75.88,

DOI: 10.1021/acs.joc.5b00342
J. Org. Chem. 2015, 80, 4501−4515

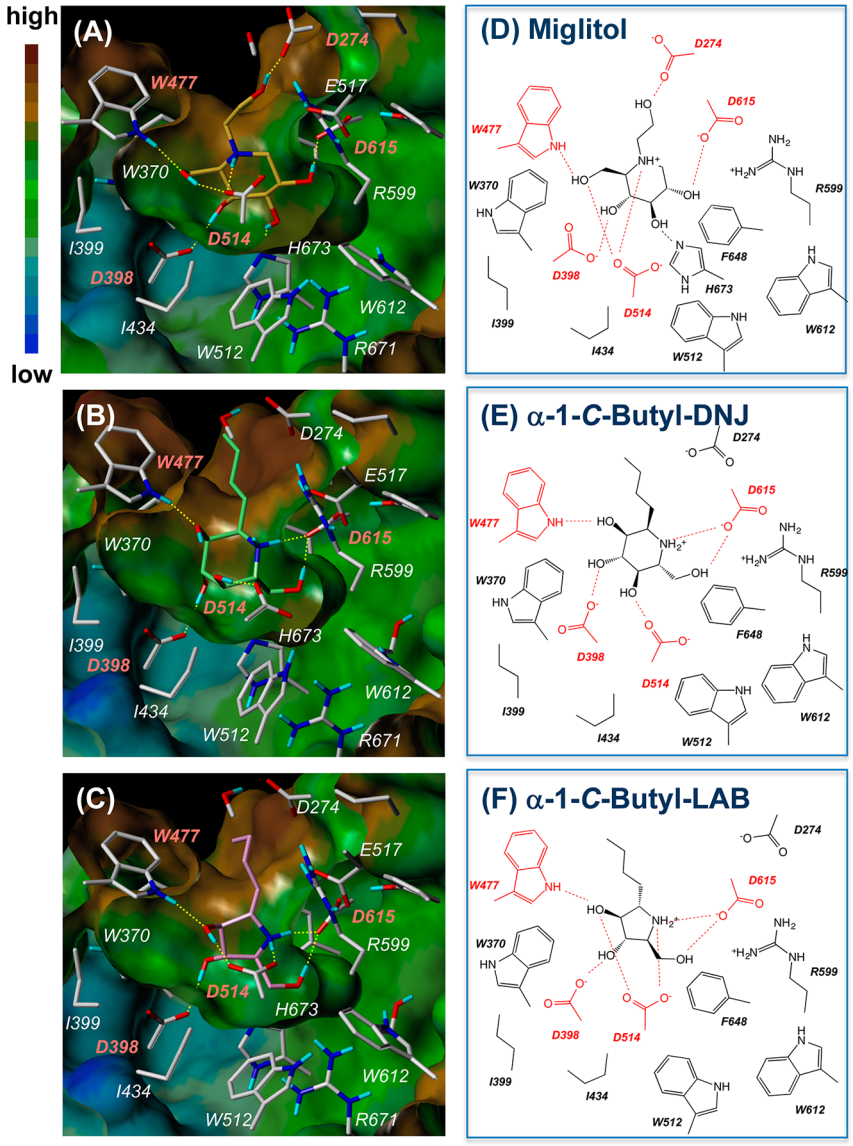

Figure 3. Binding conformations and views of interactions for rat ntSI (isomaltase). Panels A–C, binding of miglitol (A), α-1-C-butyl-DNJ (B), and α-1-C-butyl-LAB (C) in the active site of ntSI. The molecular surface of ntSI was rendered by lipophilic potential. Panels D–F, schematic diagram of hydrogen-bonding interactions and vdW interactions between ntSI and miglitol (D), α-1-C-butyl-DNJ (E), and α-1-C-butyl-LAB (F).

Table 1. Negative Logarithmic Values of Half-Maximal Inhibitory Concentration (pIC_{50}), Calculated Stabilization Energies (ΔE's), and Relative Energies ($\Delta\Delta E$'s) of Each Ligand for ntSI (Isomaltase)

	miglitol	α-1-C-butyl-DNJ	α-1-C-butyl-LAB
pIC_{50} (log μM^{-1})	4.41	6.35	5.33
ΔE (kcal/mol)	−68.89	−77.11	−75.88
$\Delta\Delta E$ (kcal/mol)	0	−8.22	−6.69

Table 2. Binding Energy Estimated for α-1-C-Butyl-LAB with Rat and Human ntSI (Isomaltase)

	ΔE (kcal/mol)
rat isomaltase	−75.88
human isomaltase	−75.44

−68.64, and −63.76 kcal/mol, respectively. These results were consistent with the experimental results (pIC_{50}) showing that of α-1-C-butyl-LAB has higher inhibitory activity against isomaltase than α-1-C-heptyl-LAB and α-1-C-nonyl-LAB, with pIC_{50} for each ligand of 5.33, 4.80, and 3.77 [log (μM^{-1})], respectively. As shown in Figure 5A, the pyrrolidine ring of α-1-C-heptyl-LAB and α-1-C-nonyl-LAB bound to ntSI (isomaltase) has the same conformation as that of α-1-C-butyl-LAB. In contrast, the binding orientation of these compounds was different from that of α-1-C-butyl-LAB. These results would indicate that ring orientation was changed due to accommodation of the long side chain in the hydrophobic pocket. As a result, the distance between NH_2^+ in the pyrrolidine ring and Phe648 was reduced from 4.32 (α-1-C-butyl-LAB) to 2.47 (α-1-C-heptyl-LAB) or 2.31 Å (α-1-C-nonyl-LAB) (Figure 5B–D), finally leading to loss of binding energies (ΔE's). These results strongly suggested that the longer α-1-C-alkyl chains reduced the inhibition activities compared to α-1-C-butyl-LAB.

Design of Labystegines. In the present study, we performed molecular dynamics (MD) calculations and found that the flexibility around the keyhole of ntSI (isomaltase) is lower than that of ctSI (sucrase) (Figure 2). Furthermore, our

DOI: 10.1021/acs.joc.5b00342
J. Org. Chem. 2015, 80, 4501–4515

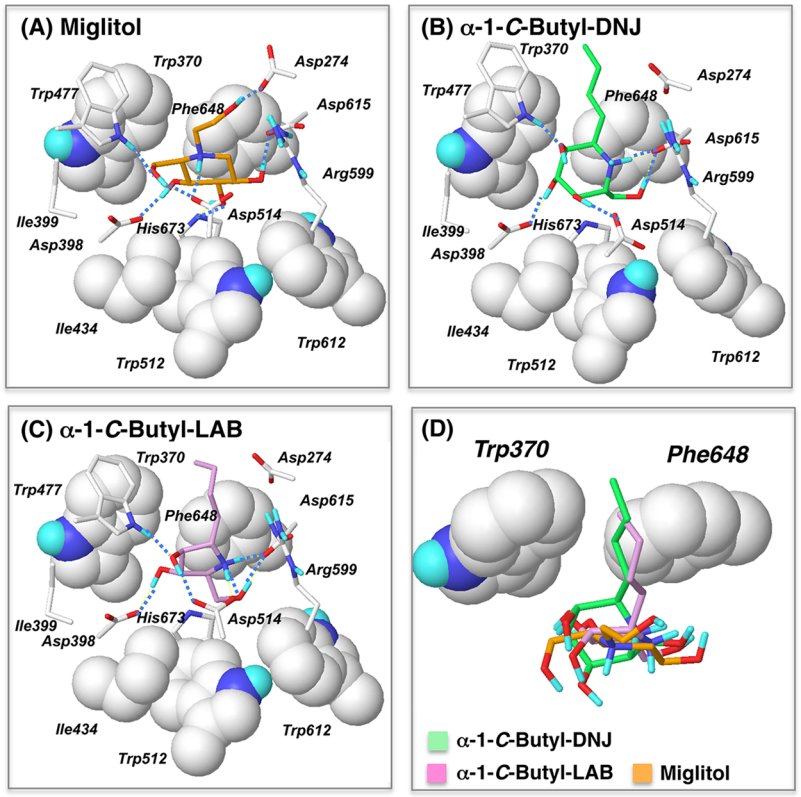

Figure 4. Binding modes of miglitol (A), α-1-*C*-butyl-DNJ (B), and α-1-*C*-butyl-LAB (C) with rat ntSI (isomaltase). The residues related to van der Waals interactions are drawn in space-filling representation. The hydrogen bonds are depicted by dashed lines. (D) Superposition of the binding conformations of miglitol, α-1-*C*-butyl-DNJ, and α-1-*C*-butyl-LAB with Trp370 and Phe648 in rat ntSI.

Table 3. Comparison of Negative Logarithmic Values of Half-Maximal Inhibitory Concentration (pIC_{50}), Calculated Stabilization Energies (ΔE's), and Relative Energies ($\Delta\Delta E$'s) for ntSI (Isomaltase) with the Length of Alkyl Groups in LAB Derivatives

	α-1-*C*-butyl-LAB	α-1-*C*-heptyl-LAB	α-1-*C*-nonyl-LAB
pIC_{50} (log μM^{-1})	5.33	4.80	3.77
ΔE (kcal/mol)	−75.88	−68.64	−63.76
$\Delta\Delta E$ (kcal/mol)	0.00	7.24	12.12

results indicated that the alkyl chain length at the anomeric position of α-1-*C*-alkyl-LAB should be limited. These results are supported by previous reports that the pseudotetrasaccharide acarbose is an efficient inhibitor of the ctMGAM (maltase) and ctSI (sucrase) but a weaker inhibitor of the ntSI (isomaltase).[9−12] In the present study, we also revealed that the binding orientation of iminosugars toward the keyhole of ntSI (isomaltase) affected the inhibition potencies: a suitable binding orientation with CH−π interaction (Trp370 and Phe648) is a requirement for achieving a strong affinity for isomaltase. On the basis of these remarkable results, we envisaged that a further improvement in activity might be gained in the case of pyrrolidine-based structures having a bicyclic ring bridge with a suitable CH−π interaction with Trp370 and Phe648. To test this hypothesis, we drew inspiration from naturally occurring calystegines to prepare a hybrid with the pyrrolidine iminosugar LAB. Calystegines are characterized as nortropane alkaloids with a high degree of hydroxylation and an unusual hemiaminal functionality at the bridge head position.[33−37] We propose that this new structural class of iminosugar with the bridge head hydroxyl group replaced by a hydroxymethyl group be named labystegine (Figure 6). The C-2, C-3, and C-4 OH groups and ring heteroatom in the six-membered ring of calystegine B_2 lie in the same region of space as the C-3, C-4 OH, and C-5 CH_2OH groups and ring heteroatom of isofagomine, respectively.[38] Furthermore, previous studies revealed that replacement of the C4 hydroxy group of 1,5-dideoxy-1,5-imino-D-xylitol (DIX) by a hydroxymethyl substituent to give isofagomine bring a dramatic increase in inhibitory potency against β-glucosidases.[39] On a similar basis, noeurostegine (C-4 hydroxymethyl calystegine B_2) was designed and subsequently shown to be a β-glucosidase inhibitor with potential as a valuable compound against Gaucher's disease.[40,41] In sharp contrast, our newly designed labystegines originate from pyrrolidine iminosugars and can be considered as α-glucosidase-inhibiting LAB derivatives with an extended bridge at the C-1 and C-4 positions. Furthermore, they differ from original calystegines in that they have a hydroxymethyl substituent instead of a hydroxy group in the bridgehead position. We envisaged that labystegine would inherit the potency and selectivity against intestinal α-glucosidases from LAB.

Synthesis of Labystegines. The nortropane scaffolds of labystegine **6** were prepared following the protocol of intramolecular [3 + 2] cycloaddition developed by Goti[30] (Scheme 1). The nitrone **1** prepared from D-xylose[42] reacted with allyl Grignard reagent to afford only a single diastereomer **2** (dr >95). The high *trans*-selectivity is in accord with previous reports.[43−46] Oxidation of hydroxylamine **2** with activated MnO_2[47,48] gave two separable regioisomers **3** and **4**. The cycloadduct **5** was obtained as the only product in high yield

DOI: 10.1021/acs.joc.5b00342
J. Org. Chem. 2015, 80, 4501−4515

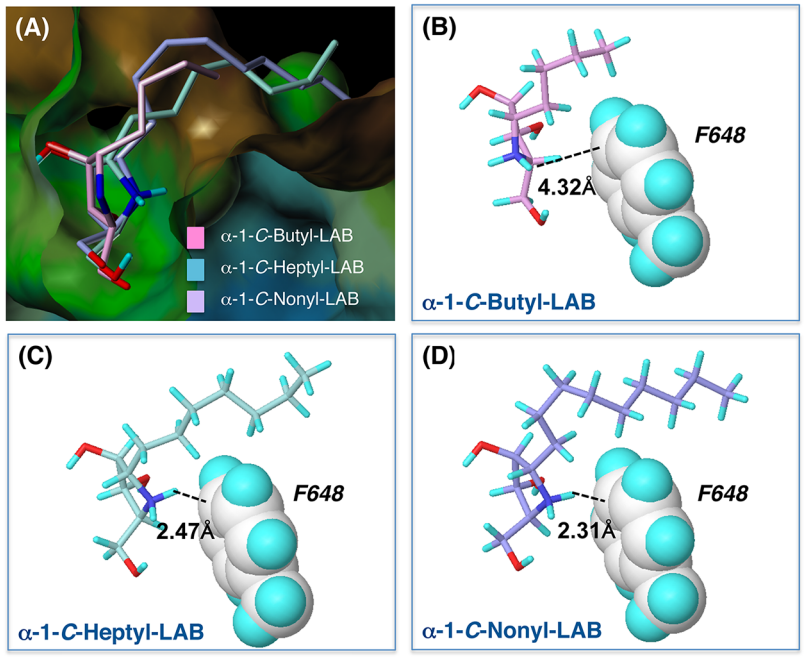

Figure 5. Binding conformations of α-1-*C*-butyl-LAB, α-1-*C*-heptyl-LAB, and α-1-*C*-nonyl-LAB for rat ntSI (isomaltase): (A) superposition of binding conformations of α-1-*C*-butyl-LAB, α-1-*C*-heptyl-LAB, and α-1-*C*-nonyl-LAB in the active site of ntSI. (B–D) Binding conformations of α-1-*C*-butyl-LAB (B), α-1-*C*-heptyl-LAB (C), α-1-*C*-nonyl-LAB (D), and Phe648 of ntSI. The numbers represent the distance between a hydrogen attached to the nitrogen of the five-membered ring and a carbon of Phe648.

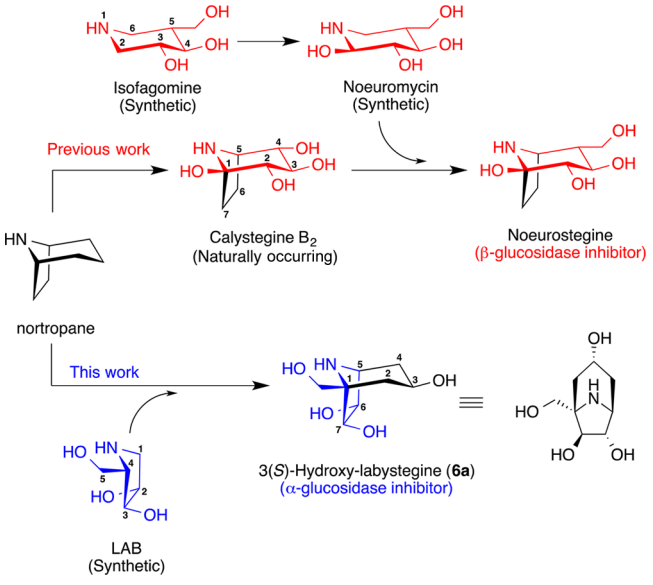

Figure 6. Design strategy of nortropane-type α-glucosidase inhibitors.

when **3** was heated in a dilute toluene solution at 120 °C for 14 h. The relative stereochemistry of the newly generated stereogenic center was confirmed by 2D NMR (NOESY and COSY) experiments. Catalytic hydrogenolysis (10% Pd/C) in acidic methanol furnished the iminosugar **6** in high yield. NMR data of compounds **2a–5a** were completely identical to those reported in ref 30.

N-Alkyl derivatives were obtained from **5a**, the N–O bond of which was then cleaved by Zn–Cu(OAc)$_2$–AcOH (Scheme 2). Subsequently, *N*-alkylation was achieved by reductive amination of aldehydes with secondary amine **7**. After Pd/C-catalyzed hydrogenolysis, *N*-alkylated iminosugars **9a,b** were obtained in high yields.

Scheme 1. Synthesis of Nortropane with [3 + 2] Cycloaddition

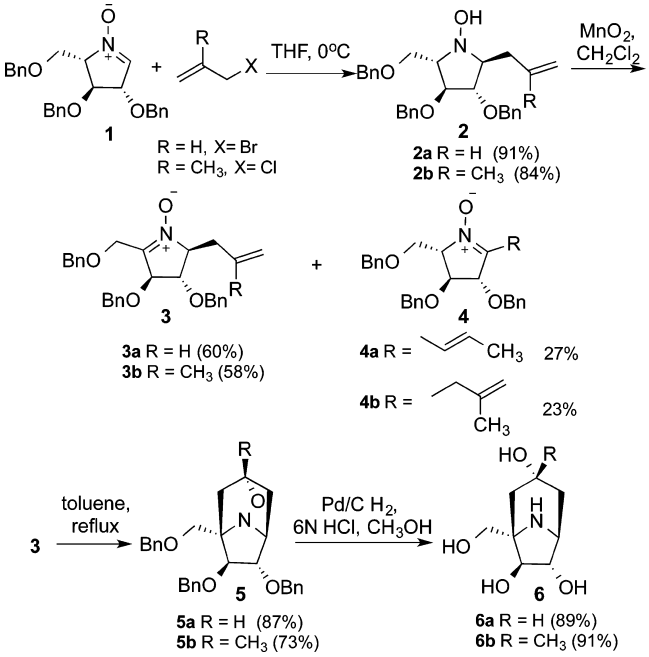

The synthesis of **16** commenced with a stereoselective nucleophilic addition of Grignard reagent to nitrone **1** to afford the hydroxylamine **11** in high yield (Scheme 3); **11** was oxidized with activated MnO_2 directly without isolation. After conversion of the acetal **12** to aldehyde **14**, the intramolecular reductive coupling reaction promoted by SmI_2[31,32,49,50] was attempted; hydroxylamine **15** was obtained as the single diastereomer. The configuration of **15** was assigned by careful analyses of 1D and 2D NMR spectra. Catalytic hydrogenolysis

DOI: 10.1021/acs.joc.5b00342
J. Org. Chem. 2015, 80, 4501–4515

Scheme 2. Synthesis of *N*-Alkyl Derivatives

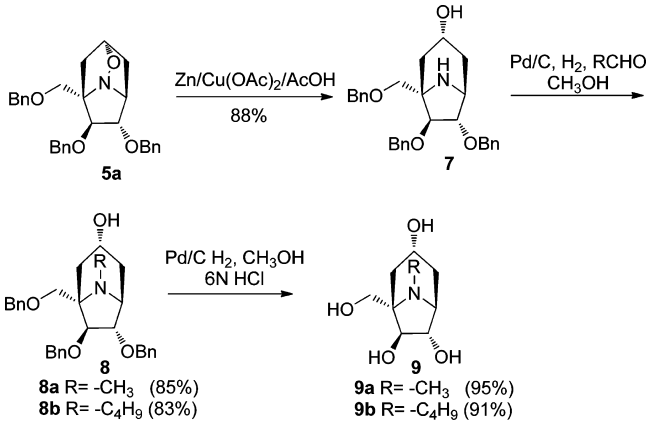

(10% Pd/C) in acidic methanol furnished the iminosugar **16** in quantitative yield.

A similar strategy (Scheme 4) was applied to synthesis of **24** which has a [2.2.1] skeleton; however, the ester bromide **17** was used as the nucleophile to afford the adduct **18**. Reduction of the lactone **18** with $LiAlH_4$, followed by oxidation by activated MnO_2, gave the key nitrone **21**. After oxidation of the alcohol **21** to the aldehyde **22**, the hydroxylamine **23** was obtained as the single diastereomer by an intramolecular reductive coupling reaction promoted by SmI_2. Catalytic hydrogenolysis (10% Pd/C) in acidic methanol afforded the iminosugar **24** in quantitative yield.

Structure–Activity Relationships of Labystegine Derivatives against Isomaltase and *β*-Glucocerebrosidase. We first investigated the inhibition potency of labystegine derivatives (Figure 7) against rat intestinal maltase, isomaltase, and sucrase. Human lysosomal *β*-glucocerebrosidase was also tested in order to extend our understanding of the selectivity against the intestinal *α*-glucosidases. The IC_{50} of labystegines, calystegines, and miglitol are shown in Table 4. Classical nortropane-type iminosugar calystegine B_2 and C_1 showed potent inhibition against *β*-glucocerebrosidase, with IC_{50} values of 5.1 and 2.8 *μ*M, whereas these calystegines exhibited less than a 50% inhibition of rat intestinal *α*-glucosidases even at concentrations as high as 1000 *μ*M. In sharp contrast, our designed **6a** was a potent inhibitor of rat intestinal maltase, isomaltase, and sucrase with IC_{50} value of 0.15, 2.8, and 0.18 *μ*M, respectively. These inhibitory potencies were 10-times better than those of miglitol. Furthermore, miglitol showed lower selectivity with inhibition of *β*-glucocerebrosidase, with an IC_{50} value of 219 *μ*M, whereas **6a** had no effect on this enzyme. Thus, we next focused on the introduction of an *N*-alkyl substituent into **6a** and whether extending the alkyl chain at this position could influence the inhibition activities of **6a** (Table 4). We found that the inhibitory potency of *N*-methyl (**9a**: IC_{50} = 254 *μ*M) and *N*-butyl derivatives (**9b**: IC_{50} = 66 *μ*M) against isomaltase were both much weaker than the parent **6a**. Furthermore, the branched *C*-methyl-compound (**6b**) also had reduced inhibitory potency against this enzyme (IC_{50} = 104 *μ*M). It is noteworthy that compound **16** kept its inhibitory potency, with IC_{50} values of 4.0 *μ*M, whereas compound **24** showed reduced inhibition (IC_{50} = 93 *μ*M) compared to compound **16**.

Docking Study of 3(*S*)-Hydroxylabystegine (6a) against ntSI. To understand the structural basis of the interaction of 3(*S*)-hydroxylabystegine (**6a**) with isomaltase, we first determined the mode of inhibition and the inhibition constant (K_i) from Lineweaver–Burk plots. We found **6a** inhibited isomaltase (ntSI) in a competitive manner, with K_i value of 0.48 *μ*M. This result suggests that **6a** occupies the active-site of this enzyme in much the same manner as miglitol. Thus, we next performed *in silico* molecular docking of this compound to rat ntSI for the purpose of understanding the increased inhibitory activity of **6a**. Figure 8 shows the binding conformation of **6a** (Figure 8A) and its interactions (Figure 8B,C) with rat ntSI. These results suggested that the binding mode of **6a** is almost same as that of *α*-1-*C*-butyl-LAB and miglitol, whereas a small difference was observed for protein–ligand interaction. The hydrogen bonds formed to Asp398, Trp477, and Asp514 of ntSI were maintained in **6a** (Figure 8B). In contrast, the bridgehead hydroxymethyl group of **6a**

Scheme 3. Synthesis of Nortropane by an Intramolecular Reductive Coupling Reaction

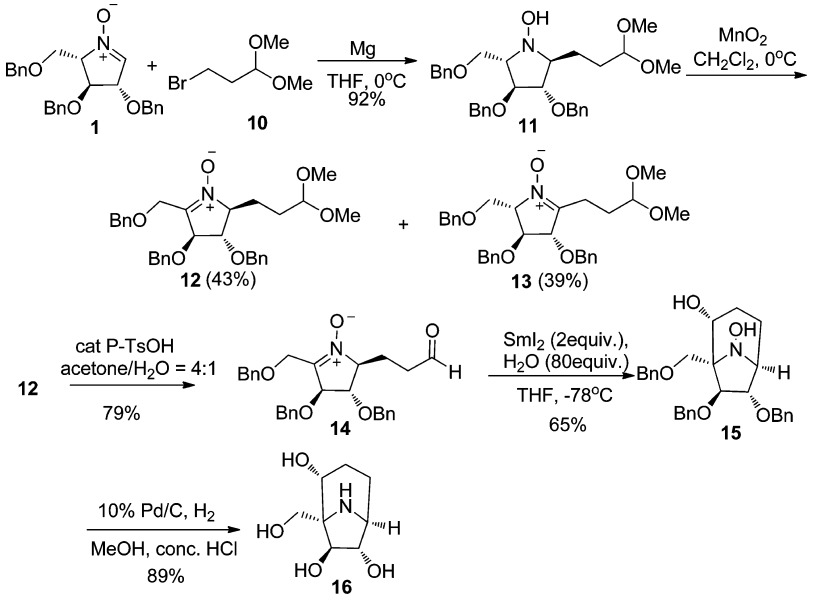

DOI: 10.1021/acs.joc.5b00342
J. Org. Chem. 2015, 80, 4501–4515

Scheme 4. Synthesis of 24 with a [2.2.1] Skeleton

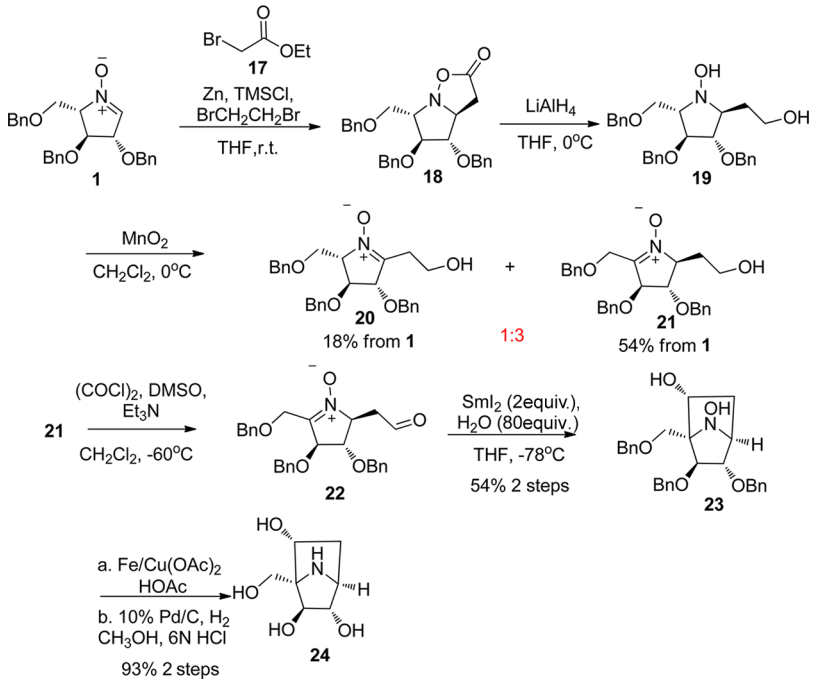

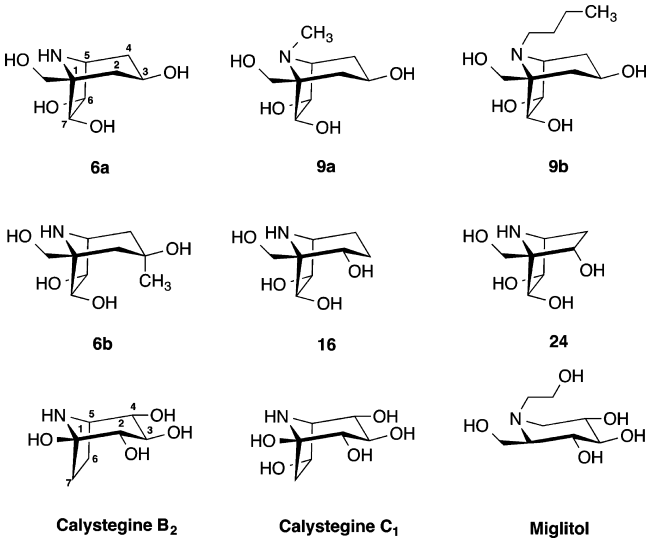

Figure 7. Chemical structures of labystegines, calystegines, and miglitol.

Table 4. IC_{50} Values (μM) for Labystegine Derivatives against Intestinal α-Glucosidases and Human Lysosome β-Glucocerebrosidase, Compared with Calystegine C_1 and Miglitol

	IC_{50} (μM)			
	rat intestinal			human lysosome
compd	maltase	isomaltase	sucrase	β-glucocerebrosidase
6a	0.15	2.8	0.18	NI[a](4.6%)[b]
9a	33	254	6.6	NI (6.1%)
9b	4.8	66	4.1	NI (6.6%)
6b	5.1	104	11	NI (3.6%)
16	1.8	4.0	0.36	NI (8.7%)
24	66	93	18	NI (3.6%)
calystegine B_2	NI (25.1%)	NI (36.8%)	385	5.1
calystegine C_1	NI (30.2%)	NI (38.8%)	319	2.8
miglitol	1.3	39	1.0	219

[a]NI: less than 50% inhibition at 1000 μM. [b]Numbers in parentheses indicate % inhibition at 1000 μM.

interacted with Asp436 and Trp477 instead of the interaction with Asp615, which was observed in α-1-C-butyl-LAB. It is noteworthy that **6a** was located closer to Trp370 than miglitol due to the van der Waals interaction between the bridge part of **6a** and the Trp370 and Phe648 of ntSI (Figure 8C, D). The hydrogen bond and van der Waals interactions may result in the increase of inhibitory activity of **6a**.

***In Vivo* Isomaltose-Loading Test.** To confirm that **6a** had significant effects on blood glucose levels *in vivo*, an isomaltose loading test was conducted using miglitol as a positive control (Figure 9). The animal experimental protocols in this study were approved by the Animal Experiments Committee of the University of Toyama. Male C57BL/6J mice (17−20 g) after an overnight fast were used for acute isomaltose loading tests. The blood glucose levels were measured by the StatStrip Xpress kit (Nova Biochemical Co. Ltd.). A control group was loaded with injection of saline only. Administration of isomaltose (2.5 g/kg body weight p.o.) to fasted mice resulted in a rapid increase in blood glucose concentrations from 74.8 ± 2.4 to a maximum of 157.0 ± 4.0 mg/dL after 60 min. A significant suppressive effect of the blood glucose level was achieved with 2.5 mg/kg body weight of 3(*S*)-hydroxylabystegine (**6a**) after 30, 60, and 120 min. A 2.5 mg/kg body weight miglitol also significantly decreased the blood glucose concentrations at 30 min after isomaltose loading. However, the suppression effects were clearly weaker than **6a**. This effect is dose-dependent, and 5.0 mg/kg body weight of **6a** showed a nearly perfect suppression effect against postprandial hyperglycemia. These results suggested that **6a** is worthy of study as a potential therapeutic agent for the treatment of diabetes.

DOI: 10.1021/acs.joc.5b00342
J. Org. Chem. 2015, 80, 4501−4515

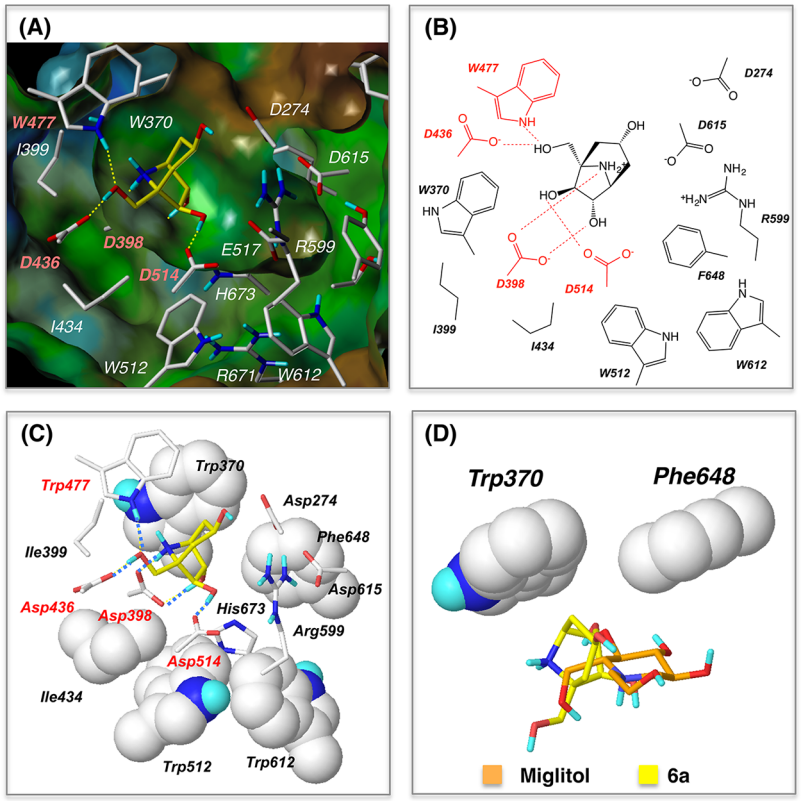

Figure 8. Binding conformations and interactions of **6a** with rat ntSI (isomaltase): (A) binding conformation of **6a** in the active site of the molecular surface rendered by lipophilic potentia; (B) schematic diagrams of hydrogen bond and van der Waals interactions of **6a**; (C) binding mode of **6a**. The residues related to van der Waals interactions are drawn in space-filling representation. The hydrogen bonds are depicted by the dashed line. (D) Superposition of the binding conformations of **6a** and miglitol with Trp370 and Phe648 in rat ntSI.

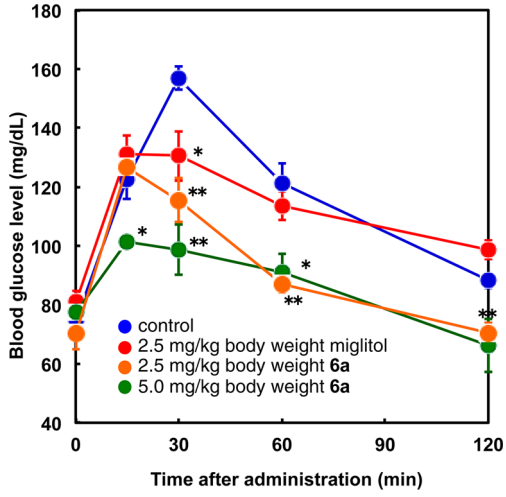

Figure 9. Effects of miglitol and **6a** on blood glucose levels. Blood glucose concentrations of male C57BL/6J mice after an oral load with isomaltose, 2.5 g/kg body weight, with (a) 2.5 (red) mg/kg body weight miglitol, (b) 2.5 (orange), and (c) 5.0 (green) mg/kg body weight **6a**. The control group was loaded with saline (blue). Each value represents the mean ± SEM ($n = 4$). **: significant difference ($p < 0.01$). *: significant difference ($p < 0.05$) compared with the control.

CONCLUSIONS

In summary, we elucidated the best molecular size and structural moieties of iminosugars for binding to the active site of ntSI (isomaltase) by molecular dynamics (MD) calculations and found that the flexibility around the keyhole of ntSI (isomaltase) is lower than that of ctSI (sucrase). Molecular docking simulations of α-glucosidase inhibitors, miglitol, α-1-C-butyl-DNJ, and α-1-C-butyl-LAB into ntSI revealed that the suitable binding orientation with CH$-\pi$ interaction (Trp370 and Phe648) is a requirement for achieving a strong affinity. The design of labystegines not only inherited suitable hydrogen bonds formed to Asp398, Trp477, and Asp514 of ntSI from LAB but also gained new CH$-\pi$ interactions with Trp370 and Phe648. It was widely accepted that nortropane iminosugars are ideally suited for the design of β-glucosidase inhibitors. However, labystegine opens up new possibilities for α-glucosidase inhibition by bridge-type bicyclic iminosugars while enhancing a designing flexibility and providing a new strategy based on inhibition moieties of the five-membered ring fragment. In particular, 3(S)-hydroxylabystegine (**6a**) showed selective intestinal maltase, isomaltase, and sucrase inhibition, and its potency was 10 times, an order of magnitude, better than that of miglitol. Furthermore, **6a** strongly suppressed postprandial hyperglycemia, similar to miglitol *in vivo*. Compound **6a** therefore represents a promising new class of a nortropane-type iminosugar that has the potential for treating postprandial hyperglycemia. Finally, the synthetic method for the preparation of labystegines is general and efficient for the synthesis of labystegine-type iminosugars and therefore is one of the very important tools for our future study on labystegines.

EXPERIMENTAL SECTION

General Experimental Procedures. All reagents were used as received from commercial sources without further purification or

DOI: 10.1021/acs.joc.5b00342
J. Org. Chem. 2015, 80, 4501−4515

prepared as described in the literature. Tetrahydrofuran was distilled from sodium and benzophenone immediately before use. Reactions were stirred using Teflon-coated magnetic stirring bars. Analytical TLC was performed with 0.20 mm silica gel 60F plates with 254 nm fluorescent indicator. TLC plates were visualized by ultraviolet light or by treatment with a spray of Pancaldi reagent [$(NH_4)_6MoO_4$, $Ce(SO_4)_2$, H_2SO_4, H_2O] or a solution 0.5% ninhydrin in acetone. Chromatographic purification of products was carried out by flash column chromatography on silica gel (230−400 mesh). Acidic ion-exchange chromatography was performed on Amberlite IR-120 (H^+) or Dowex 50WX8-400, H^+ form. Melting points were determined using an electrothermal melting point apparatus. Both melting points and boiling points are uncorrected. Infrared spectra were recorded on an FT/IR-480 plus Fourier transform spectrometer. NMR spectra were measured in $CDCl_3$ (with TMS as internal standard) or D_2O on a 300 M (^{1}H at 300 MHz, ^{13}C at 75 MHz), 400 M (^{1}H at 400 MHz, ^{13}C at 100 MHz), or 600 M (^{1}H at 600 MHz, ^{13}C at 150 MHz) NMR spectrometer. Chemical shifts (δ) are reported in ppm, and coupling constants (J) are reported in Hz. The following abbreviations were used to explain the multiplicities: s = singlet, d = doublet, t = triplet, q = quartet, m = multiplet. High-resolution mass spectra (HRMS) were recorded on a LTQ/FT mass spectrometer or a GCT mass spectrometer. Polarimetry was carried out using an AA-10R polarimeter, and the measurements were made at the sodium D line with a 0.5 dm path length cell. Concentrations (c) are given in grams per 100 mL.

Synthesis of 3(*S*)-Hydroxylabstegine (6a). *(2S,3S,4S,5S)-1-Hydroxy-2-allyl-3,4-bis(benzyloxy)-5-(benzyloxymethyl)pyrrolidine (**2a**).* A solution of allylmagnesium bromide in Et_2O (1 M, 9.6 mL) was slowly added by syringe under argon to a cooled (0 °C) solution of nitrone **1** (1 g, 2.4 mmol) in THF; the resulting reaction mixture was stirred for 30 min, quenched with aq NH_4Cl, and allowed to warm to room temperature. The aqueous layer was extracted with ethyl acetate, the combined extracts were dried, and the solvents were removed in vacuo. The residue was purified by flash chromatography (EtOAc/petroleum ether, 1:2) to give the title compound **2a** as a colorless oil (947 mg, 86%): R_f = 0.73 (EA/PE = 1:2); $[\alpha]_D^{20}$ +3.4 (c 0.48 CH_2Cl_2); IR (KBr, film) ν 3243, 3067, 3032, 2867, 1639, 1490, 1452, 1363, 1305, 1208, 1100, 914 cm^{-1}; ^{1}H NMR (300 MHz $CDCl_3$) δ 7.29−7.16 (m, 15H, Ph), 7.06 (br, 1H, OH), 5.83−5.78 (m, 1H, H-8), 5.09−5.02 (m, 2H, H-9), 4.53−4.41 (m, 6H, CH_2Ph), 3.95 (dd, J = 2.4, 3.9 Hz, 1H, H-4), 3.83−3.75 (m, 2H, H-3, H-6), 3.62 (dd, J = 6.6, 9.0 Hz, 1H, H-6), 3.51−3.46 (m, 1H, H-5), 3.33−3.27 (m, 1H, H-2), 2.74−2.65 (m, 1H, H-7), 2.33−2.23 (m, 1H, H-7); ^{13}C NMR (75 MHz $CDCl_3$) δ 138.31, 138.25 (Ph), 135.6 (C-8), 128.39, 128.37, 127.94, 127.90, 127.8, 127.7 (Ph), 117.0 (C-9), 85.5 (C-3), 84.3 (C-4), 73.4, 71.7 (CH_2Ph), 69.9 (C-5), 69.4 (C-2), 68.4 (C-6), 32.7 (C-7); DEPT-135 (75 MHz CDCl3) δ positive: 135.6, 128.4, 128.0, 127.9, 127.8, 127. 7, 127.6, 85.5, 84.3, 69.9, 69.4, negative: 117.0, 73.4, 71.7, 32.7; HRMS (EI) m/z calcd for $C_{29}H_{33}NO_4[M]^+$ 459.2410• found 459.2413.

*(3S,4S,5S)-2-(Benzyloxymethyl)-3,4-bis(benzyloxy)-5-allyl-1-pyrroline N-Oxide (**3a**) and (3S,4S,5S)-2-((E)-Prop-1-en-1-yl)-3,4-bis-(benzyloxy)-5-(benzyloxymethyl)-1-pyrroline N-Oxide (**4a**).* Activated manganese dioxide (0.38 g, 4.36 mmol) was added portionwise to a cooled (0 °C) solution of hydroxylamine **2a** (1 g, 2.18 mmol) in CH_2Cl_2. The suspension was stirred at room temperature for 12 h. The resultant mixture was filtered with Celite and concentrated in vacuo. The crude product was purified by flash chromatography to give the title compound **3a** as a colorless oil (600 mg, 60%) and **4a** also as a colorless oil (270 mg, 27%): **3a** $[\alpha]_D^{20}$ +53.3 (c 3.15, CH_2Cl_2); IR (cm^{-1}) 3033, 2916, 2865, 1722, 1590, 1494, 1451, 1361, 1248, 1210, 1009, 920; ^{1}H NMR (300 MHz, $CDCl_3$) δ 7.31−7.26 (m, 15H, Ph), 5.76−5.68 (m, 1H, H-8), 5.14−5.09 (m, 2H, H-9), 4.70−4.51 (m, 6H, H-3, H-6, CH_2Ph), 4.42−4.33 (m, 3H, H-6, CH_2Ph), 3.98 (d, J = 6.9 Hz, 1H, H-5), 3.87 (s, 1H, H-4), 2.94−2.89 (m, 1H, H-7), 2.51−2.44 (m, 1H, H-7); ^{13}C NMR (75 MHz $CDCl_3$) δ 142.6 (C-2), 137.5, 137.1 (Ph), 132.5 (C-8), 128.6, 128.5, 128.1, 128.03, 127.97, 127.8 (Ph), 119.2 (C-9), 82.9 (C-3), 79.9 (C-4), 78.5 (C-5), 73.6, 72.5, 71.4 (CH_2Ph), 62.7 (C-6), 35.4 (C-7); HRMS (ESI) m/z calcd for $[C_{29}H_{31}NO_4H^+]$ 458.2326, found 458.2326. **4a**: $[\alpha]_D^{20}$ +29.1 (c 3.30, CH_2Cl_2); IR (cm^{-1}) 3033, 2866, 1721, 1543, 1452, 1363, 1212, 1094; ^{1}H NMR (300 MHz, $CDCl_3$) δ 7.31−7.18 (m, 15H, Ph), 6.62−6.51 (m, 2H, H-7, H-8), 4.84 (s, 1H, H-4), 4.64−4.45 (m, 6H, 3 × CH_2Ph), 4.27 (s, 1H, H-5), 4.09 (s, 1H, H-3), 4.01 (dd, J = 6.0, 9.9 Hz, 1H, H-6), 3.88 (dd, J = 2.7, 9.6 Hz, 1H, H-6), 1.87 (d, J = 5.4 Hz, 3H, H-9); ^{13}C NMR (75 MHz $CDCl_3$) δ 147.8 (C-2), 137.7, 137.3, 137.2 (Ph), 137.2 (C-7), 128.6, 128.5, 128.4, 127.1, 128.1, 128.0, 127.9, 127.8 (Ph), 118.9 (C-8), 83.5 (C-4), 78.2 (C-3, C-5), 73.6, 71.5, 70.4 (CH_2Ph), 67.4 (C-6), 19.5 (b C-9); HRMS (EI) m/z calcd for $[C_{29}H_{31}NO_4^+]$ 457.2253, found 457.2257.

(1R,3S*,4S*,5S*,6S*)-3-(Benzyloxymethyl)-4,5-bis(benzyloxy)-7-aza-8-oxytricyclo[4.2.1.0^{3,7}]nonane (**5a**).* A solution of nitrone **3a** (195 mg, 0.43 mmol) was dissolved in anhydrous toluene and heated at reflux under an argon atmosphere. After the reaction was completed, the solvent was evaporated and the resulting crude product was purified by flash chromatography to give the title compound **5a** as yellow light oil (170 mg, 87%): $[\alpha]_D^{20}$ +27.6 (c 3.48, CH_2Cl_2); IR (cm^{-1}) 3062, 3029, 2981, 2947, 2862, 1495, 1453, 1361, 1300, 1254, 1209, 1105, 1026; ^{1}H NMR (300 MHz $CDCl_3$) δ 7.40−7.22 (m, 15H, PhH), 4.74−4.70 (m, 2H, H-1, CH_2Ph), 4.59−4.43 (m, 5H, CH_2Ph), 4.34 (d, J = 1.5 Hz, 1H, H-5), 3.90 (d, J= 2.4 Hz, 1H, H-4), 3.63 (dd, J = 2.1, 10.2 Hz, 1H, H-6), 3.52 (d, J = 10.2 Hz, 1H, H-9), 3.35 (d, J = 10.2 Hz, 1H, H-9), 2.22−2.12 (m, 1H, H-7), 1.98 (d, J = 12.3 Hz, 1H, H-2), 1.44−1.37 (m, 2H, H-2, H-7); ^{13}C NMR (75 MHz, $CDCl_3$) δ 138.4, 138.2, 137.9 (Ph), 128.44, 128.35, 128.33, 127.9, 127.9, 127.8, 127.7, 127.5 (Ph), 86.9 (C-4), 83.1 (C-5), 79.0 (C-1), 76.8 (C-3), 72.3 (C-9), 73.6, 72.9, 71.4 (CH_2Ph), 67.3 (C-6), 39.7 (C-7), 37.1(C-2); HRMS (EI) m/z calcd for $[C_{29}H_{31}NO_4^+]$ 457.2256, found 457.2253.

*(1S,3R,5S,6S,7S)-1-(Hydroxymethyl)-8-azabicyclo[3.2.1]octane-3,6,7-triol (**6a**).* 10% Pd/C (30 mg) and concd HCl (1 mL) were added to a solution of cycloadduct **5a** (90 mg, 0.20 mmol) in MeOH. The mixture was stirred under an atmosphere of H_2 at room temperature for 16 h when the cycloadduct was judged to diminish by TLC, and then Ar was bubbled through the reaction mixture and the Pd/C was filtered off. The solvent was removed under reduced pressure, and $NH_3{\cdot}H_2O$ (25%, 10 mL) was added. After being stirred for 10 min, the solvent was removed under reduced pressure and the residue was purified by acid ion-exchange resin column (Dowex 50WX8−400, H^+ form) to give **6a** as yellow oil (33 mg, 89%): $[\alpha]_D^{20}$ +0 (c 1.66, MeOH); IR (cm^{-1}) 3343, 2935, 1091, 1052; ^{1}H NMR (300 MHz, D_2O) δ 4.04−3.93 (m, 2H, H-4, H-7), 3.86 (s, 1H, H-6), 3.48 (s, 2H, H-8), 3.12 (s, 1H, H-5), 2.11−2.07 (m, 1H, H-4), 1.98 (q, J = 6.0 Hz, 1H, H-2), 1.50−1.41 (m, 1H, H-4), 1.31 (t, J = 12.3 Hz, 1H, H-2); ^{13}C NMR (75 MHz, D_2O) δ 81.8 (C-6), 81.1 (C-7), 66.1 (C-1), 63.8 (C-8), 63.0 (C-3), 60.6 (C-5), 36.6 (C-4), 35.3 (C-2); m/z calcd for $[C_8H_{15}NO_4H^+]$ 190.1074, found 190.1073.

Synthesis of 3(*S*)-3-Hydroxy-3-methyllabystegine (6b). *(2S,3S,4S,5S)-1-Hydroxy-2-(benzyloxymethyl)-3,4-bis(benzyloxy)-5-(2-methylallyl)pyrrolidine (**2b**).* A solution of (2-methylallyl)-magnesium bromide in THF (1 M, 9.6 mL) was slowly added by syringe under argon to a cooled (0 °C) solution of nitrone **1** (1 g, 2.4 mmol) in THF; the resulting reaction mixture was stirred for 30 min, quenched with aq NH_4Cl, and allowed to warm to room temperature. The aqueous layer was extracted with ethyl acetate, the combined extracts were dried, and the solvents were removed in vacuo. The residue was purified by flash chromatography (EtOAc/petroleum ether, 1:2) to give the title compound **2b** as a colorless oil (1.16g, 91%): $[\alpha]_D^{20}$ −27 (c 1.05, $CHCl_3$); IR (KBr, film) ν 3239, 3065, 3030, 2915, 2862, 1646, 1495, 1453, 1362, 1307, 1206, 1177, 1098, 1027, 892, 818, 736, 696 cm^{-1}; ^{1}H NMR (300 MHz $CDCl_3$) δ 7.31−7.24 (m, 15H, PhH), 6.19 (br, 1H, OH), 4.79 (d, J = 8.7 Hz, 2H, H-9), 4.57−4.37 (m, 6H, 6 × CH_2Ph), 3.93−3.92 (m, 1H, H-4), 3.84−3.83 (m, 1H, H-3), 3.80 (dd, J = 5.1, 9.6 Hz, 1H, H-6), 3.63 (dd, J = 6.6, 9.0 Hz, 1H, H-6), 3.53−3.42 (m, 2H, H-2, H-5), 2.69 (dd, J = 5.4, 13.8 Hz, 1H, H-7), 2.27 (dd, J = 9.3, 14.1 Hz, 1H, H-7), 1.75 (s, 3H, H-10); ^{13}C NMR (75 MHz $CDCl_3$) δ 143.2 (C-8), 138.2, 138.12, 138.08, 128.37, 128.36, 128.32, 128.0, 127.9, 127.71, 127.68, 127.65, 127.61, 112.7 (C-9), 85.9 (C-4), 84.3 (C-3), 73.3, 71.6, 71.6, 70.0 (C-2), 68.6

DOI: 10.1021/acs.joc.5b00342
J. Org. Chem. 2015, 80, 4501−4515

(C-6), 68.0 (C-5), 35.9 (C-7), 22.5 (C-10); HRMS (ESI) m/z calcd for $[C_{35}H_{35}NO_4H^+]$ 534.2639, found 534.2643.

*(3S,4S,5S)-2-(Benzyloxymethyl)-3,4-bis(benzyloxy)-5-(2-methylallyl)-1-pyrroline N-Oxide (**3b**) and (3S,4S,5S)-2-(2-Methylallyl)-3,4-bis(benzyloxy)-5-(benzyloxymethyl)-1-pyrroline N-Oxide (**4b**).* The reaction of activated manganese dioxide (184 mg, 2.12 mmol) and hydroxylamine **2b** (500 mg, 1.06 mmol) gave **3b** as colorless oil (290 mg, 58%) and **4b** also as a colorless oil (115 mg, 23%). **3b**: $[\alpha]_D^{20}$ +70.0 (c 1.0, CH_2Cl_2); IR (cm^{-1}) 3063, 3031, 2917, 2863, 1649, 1587, 1496, 1453, 1358, 1246, 1208, 1092, 1069, 1028, 901, 739, 698; ^{1}H NMR (300 MHz, $CDCl_3$) δ 7.32−7.21 (m, 15H, PhH), 4.84 (s, 1H, H-9), 4.73−4.52 (m, 7H, H-6, H-9, H-3, 4 × CH_2Ph), 4.39−4.32 (m, 3H, H-6, 2 × CH_2Ph), 4.08 (d, J = 9.0 Hz, 1H, H-5), 3.88 (s, 1H, H-4), 3.04 (dd, J = 2.7, 14.1 Hz, 1H, H-7), 2.34 (dd, J = 12, 14.1 Hz, 1H, H-7), 1.76 (s, 3H, H-10); ^{13}C NMR (75 MHz, $CDCl_3$) δ142.3 (C-2), 141.0 (C-8), 137.52, 137.48, 137.2, 128.6, 128.5, 128.5, 128.2, 128.10, 128.07, 128.04, 127.99, 127.8, 114.1 (C-9), 82.6 (C-3), 80.0 (C-4), 78.1 (C-5), 73.6, 72.5, 71.3, 62.96 (C-6), 39.7 (C-7), 22.4 (C-10); HRMS (ESI) m/z calcd for $[C_{30}H_{33}NO_4Na^+]$ 494.2302, found 494.2298 (−0.81 ppm). **4b** $[\alpha]_D^{20}$ +68 (c 1.0, CH_2Cl_2); IR (cm^{-1}) 3062, 3031, 2911, 2865, 1650, 1590, 1523, 1496, 1453, 1364, 1256, 1209, 1092, 1073, 1027, 901, 818, 738, 698; ^{1}H NMR (300 MHz, $CDCl_3$) δ 7.33−7.22 (m, 15H, PhH), 4.82 (s, 1H, H-9), 4.74 (s, 1H, H-9), 4.60−4.45 (m, 7H, 6 × CH_2Ph, H-3), 4.23−4.22 (m, 1H, H-4), 4.10−4.09 (m, 1H, H-5), 4.02 (dd, J = 6.0, 10.2 Hz, 1H, H-6), 3.85 (dd, J = 3.0, 9.9 Hz, 1H, H-6), 3.46 (d, J = 15.0 Hz, 1H, H-7), 3.06 (d, J = 15.0 Hz, 1H, H-7), 1.74 (s, 3H, H-10); ^{13}C NMR (75 MHz, $CDCl_3$) δ 144.3 (C-8), 139.3 (C-2), 137.8, 137.4, 137.2, 128.6, 128.52, 128.46, 128.40, 128.1, 128.04, 127.98, 127.9, 127. 8, 113.4 (C-9), 84.5 (C-3), 78.2 (C-5), 77.7 (C-4), 73.5, 71.8, 71.7, 67.0 (C-6), 32.9 (C-7), 23.0 (C-10); HRMS (ESI) m/z calcd for $[C_{30}H_{33}NO_4Na^+]$ 494.2302, found 494.2298 (−0.77 ppm).

(1R,3S*,4S*,5S*,6S*)-1-Methyl-3-(benzyloxymethyl)-4,5-bis(benzyloxy)-7-aza-8-oxytricyclo[4.2.1.0^{3,7}]nonane (**5b**).* Compound **5b** was obtained as a colorless oil (146 mg, 73%): $[\alpha]_D^{20}$ +29.1 (c 0.55, CH_2Cl_2); IR (cm^{-1}) 3062, 3030, 2929, 2868, 1496, 1453, 1384, 1361, 1208, 1097, 1028, 909, 832, 737, 698; ^{1}H NMR (300 MHz, $CDCl_3$) δ 7.32−7.23 (m, 15H, PhH), 4.75−4.43 (m, 6H, 6 × CH_2Ph), 4.32 (s, 1H, H-5), 3.90 (d, J = 2.1 Hz, 1H, H-4), 3.77 (d, J = 10.2 Hz, 1H, H-6), 3.56 (d, J = 10.2 Hz, 1H, H-10), 3.38 (d, J = 10.5 Hz, 1H, H-10), 2.12 (J = 12.3 Hz, 1H, H-2), 2.05 (td, J = 3.3, 11.1 Hz, 1H, H-9), 1.53−1.50 (m, 4H, H-9, H-11), 1.26 (dd, 1H, H-2); ^{13}C NMR (75 MHz, $CDCl_3$) δ138.5, 138.3, 137.9, 128.4, 128.31, 128.29, 127.9, 127.8, 127.73, 127.67, 127.64, 127.5, 87.6 (C-1), 87.0 (C-4), 83.6 (C-5), 78.3 (C-3), 73.5, 73.1, 72.2, 71.3 (C-10), 69.1 (C-6), 45.0 (C-9), 42.6 (C-2), 17.1 (C-11); HRMS (ESI) m/z calcd for $[C_{30}H_{33}NO_4Na^+]$ 494.2302, found 494.2296 (−1.21 ppm).

*(1S,3R,5S,6S,7S)-1-(Hydroxymethyl)-3-methyl-8-azabicyclo[3.2.1]octane-3,6,7-triol (**6b**).* Compound **6b** was obtained as a colorless oil (70 mg, 91%): $[\alpha]_D^{20}$ +44.4 (c 1.26, MeOH); IR (cm^{-1}) 3355, 2938, 1217, 1061; ^{1}H NMR (300 MHz, D_2O) δ 4.09 (d, J = 3.3 Hz, 1H, H-7), 4.05 (d, J = 3.0 Hz, 1H, H-6), 3.47−3.35 (m, 3H, H-5, 2 × H-8), 2.06 (dd, J = 3.3, 12.0 Hz, 1H, H-4), 1.96 (d, J = 12.9 Hz, 1H, H-2), 1.70 (dd, J = 2.7, 12.3 Hz, 1H, H-4), 1.43 (s, 3H, H-9), 1.27 (dd, J = 3.3, 12.9 Hz, 1H, H-2); ^{13}C NMR (75 MHz, D_2O) δ 89.2 (C-3), 80.7 (C-6), 79.0 (C-1), 76.5 (C-7), 71.8 (C-5), 63.1 (C-8), 44.7 (C-4), 40.2 (C-2), 15.9 (C-9); HRMS (ESI) m/z calcd for $[C_9H_{17}NO_4H^+]$ 204.1230, found 204.1233 (1.05 ppm).

Synthesis of *N*-Alkyl-3(*S*)-hydroxylabystegines. *(1S,3R,5S,6S,7S)-6,7-Bis(benzyloxy)-1-((benzyloxy)methyl)-8-azabicyclo[3.2.1]octan-3-ol (**7**).* Copper(II) acetate (132 mg, 0.66 mmol) was added to a suspension of Zn powder (4.29 g, 66 mmol) in acetic acid (20 mL), and the mixture was stirred at room temperature for 2 h after which the color turned to brown. A solution of **5a** (3 g, 6.6 mmol) in AcOH (20 mL) was added, the reaction mixture was stirred at room temperature for 3 h, and acetic acid was removed under reduced pressure. The residue was dissolved in ethyl acetate, the pH adjusted to 8 by addition of aqueous solution of $NaHCO_3$, and the mixture was filtered with Celite. The filtrate was extracted with ethyl acetate (3 × 30 mL), and the combined organic layers were dried (Na_2SO_4) and concentrated at reduced pressure. The residue was purified by flash column chromatography (silica gel, petroleum ether/AcOEt 1/1) to afford amine 7 as a colorless solid (2.64 g, 88%): mp 123−124 °C; $[\alpha]_D^{20}$ + 4.0 (c 1.0, $CHCl_3$); IR (cm^{-1}) 3235, 3026, 2944, 2885, 1496, 1452, 1391, 1361, 1214, 1126, 1092, 1072, 885, 755, 738, 696; ^{1}H NMR (300 MHz, $CDCl_3$) δ 7.32−7.22 (m, 15H), 4.55−4.32 (m, 6H), 4.11−4.00 (m, 1H), 3.97 (s, 1H), 3.76−3.75 (d, J = 1.5 Hz, 1H), 3.41−3.30 (m, 3H), 2.62 (br, 2H), 2.06−1.96 (m, 2H), 1.61−1.52 (m, 1H), 1.27 (t, J = 11.2 Hz, 1H); ^{13}C NMR (75 MHz, $CDCl_3$) δ138.4, 138.2, 138.0, 128.5, 128.41, 128.37, 128.0, 127.8, 127.3, 88.5, 88.4, 73.3, 72.9, 72.7, 71.2, 64.7, 64.1, 57.9, 39.4, 38.6; HRMS (ESI) m/z calcd for $[C_{29}H_{33}NO_4H^+]$ 460.2488, found 460.2483.

Synthesis of 3(*S*)-Hydroxy-*N*-methyllabystegine (9a). *(1S,3R,5S,6S,7S)-6,7-Bis(benzyloxy)-1-((benzyloxy)methyl)-8-methyl-8-azabicyclo[3.2.1]octan-3-ol (**8a**).* To a solution of 7 (138 mg, 0.3 mmol) in CH_3OH (10 mL) were added 40% HCHO (67.5 mg, 0.9 mmol) and 10% Pd/C (30 mg), the mixture was stirred under an atmosphere of H_2 at room temperature for 16 h, the flask was bubbled with Ar, and the Pd/C was filtered off. The solvent was removed under reduced pressure, and the residue was purified by flash column chromatography (silica gel, petroleum ether/AcOEt 3/1) to afford **8a** as a colorless oil (121 mg, 85%): $[\alpha]_D^{20}$ + 12.0 (c 1.9, $CHCl_3$); IR (cm^{-1}) 3378, 3030, 2933, 2860, 1662, 1496, 1454, 1308, 1073, 1039, 737, 700; ^{1}H NMR (300 MHz, $CDCl_3$) δ 7.34−7.18 (m, 15H), 4.62 (d, J = 12.3 Hz, 1H), 4.52−4.35 (m, 5H), 3.95−3.91 (m, 1H), 3.85 (s, 1H), 3.57 (s, 1H), 3.32 (s, 3H), 2.40 (s, 3H), 1.82 (br, 1H), 1.77−1.65 (m, 2H), 1.56−1.45 (m, 2H); ^{13}C NMR (75 MHz, $CDCl_3$) δ 138.4, 138.3, 138.0, 128.2, 128.1, 127.7, 127.6, 127.50, 127.46, 127.42, 87.7, 85.5, 77.4, 73.2, 72.2, 72.1, 71.2, 65.3, 64.0, 63.2, 31.2, 30.0, 29.2; HRMS (ESI) m/z calcd for $[C_{30}H_{35}NO_4H^+]$ 474.2639, found 474.2638.

*(1S,3R,5S,6S,7S)-1-(Hydroxymethyl)-8-methyl-8-azabicyclo-[3.2.1]octane-3,6,7-triol (**9a**).* Compound **9a** was obtained as a yellow oil (49 mg, 95%): $[\alpha]_D^{20}$ −4.0 (c 2.0, MeOH); IR (cm^{-1}) 3348, 2938, 1470, 1301, 1173, 1130, 1095, 1041, 727; ^{1}H NMR (400 MHz, D_2O) δ 3.96−3.91 (m, 1H), 3.88 (d, J = 3.0 Hz, 2H), 3.55 (d, J = 12.5 Hz, 1H), 3.51 (d, J = 12.6 Hz, 1H), 3.12 (s, 1H), 2.35 (s, 3H), 1.79−1.76 (m, 2H), 1.68 (dd, J = 6.3, 13.5 Hz, 1H), 1.48 (t, J = 11.1 Hz, 3H); ^{13}C NMR (100 MHz, D_2O) δ 80.7, 79.1, 67.2, 66.7, 62.9, 62.4, 30.3, 28.7, 27.4; HRMS (ESI) m/z calcd for $[C_9H_{17}NO_4H^+]$ 204.1230, found 204.1232 (1.05 ppm).

Synthesis of *N*-Butyl-3(*S*)-hydroxylabystegine (9b). *(1S,3R,5S,6S,7S)-6,7-Bis(benzyloxy)-1-((benzyloxy)methyl)-8-butyl-8-azabicyclo[3.2.1]octan-3-ol (**8b**).* To a solution of 7 (138 mg, 0.3 mmol) in CH_3OH (10 mL) were added butyraldehyde (65 mg, 0.9 mmol) and 10% Pd/C (30 mg), the mixture was stirred under an atmosphere of H_2 at room temperature for 16 h, the flask was bubbled with Ar, and the Pd/C was filtered off. The solvent was removed under reduced pressure, and the residue was purified by flash column chromatography (silica gel, petroleum ether/AcOEt 5/1) to afford **8b** as a colorless oil (128 mg, 83%): $[\alpha]_D^{20}$ + 22.0 (c 1.6, $CHCl_3$); IR (cm^{-1}) 3403, 3028, 2930, 2858, 1496, 1454, 1362, 1100, 1072, 735, 697; ^{1}H NMR (300 MHz, $CDCl_3$) δ 7.35−7.18 (m, 15H), 4.61 (d, J = 12.2 Hz, 1H), 4.50−4.39 (m, 5H), 4.01−3.90 (m, 1H), 3.80 (s, 1H), 3.58 (d, J = 2.1 Hz, 1H), 3.41 (s, 1H), 3.37 (d, J = 9.9 Hz, 1H), 3.32 (d, J = 9.9 Hz, 1H), 2.63 (t, J = 7.0 Hz, 2H), 1.74−1.25 (m, 9H), 0.91 (t, J = 7.2 Hz, 3H); ^{13}C NMR (75 MHz, $CDCl_3$) δ 138.43, 138.38, 138.2, 128.3, 128.22, 128.15, 128.0, 127.7, 127.6, 127.4, 87.6, 85.4, 77.4, 73.1, 72.7, 72.1, 71.2, 65.7, 64.2, 58.6, 42.5, 30.2, 30.0, 29.6, 20.8, 14.1; HRMS (ESI) m/z calcd for $[C_{33}H_{41}NO_4H^+]$ 516.3108, found 516.3104.

(1S,3R,5S,6S,7S)-8-Butyl-1-(hydroxymethyl)-8-azabicyclo[3.2.1]-octane-3,6,7-triol. Compound **9b** was obtained as a yellow oil (55 mg, 91%): $[\alpha]_D^{20}$ +30.0 (c 1.8, MeOH); IR (cm^{-1}) 3359, 2934, 1456, 1377, 1300, 1160, 1096, 1022, 723; ^{1}H NMR (400 MHz, D_2O) δ 3.98−3.90 (m, 1H), 3.87 (s, 2H), 3.58 (d, J = 12.2 Hz, 1H), 3.52 (d, J = 12.3 Hz, 1H),3.30 (s, 1H), 2.75−2.70 (m, 1H), 2.55−2.50 (s, 1H), 1.79−1.66 (m, 3H), 1.39−1.33 (m, 3H), 0.91 (t, J = 7.2 Hz, 3H); ^{13}C NMR (100 MHz, D_2O) δ 80.9, 79.0, 67.3, 63.1, 62.8, 62.0, 42.2, 28.4,

DOI: 10.1021/acs.joc.5b00342
J. Org. Chem. 2015, 80, 4501−4515

28.1, 27.7, 20.3, 13.3; HRMS (ESI) m/z calcd for $[C_{12}H_{23}NO_4H^+]$ 246.1700, found 246.1699.

Synthesis of 2(*R*)-Hydroxylabystegine (16). *(2S,3S,4S,5S)-1-Hydroxy-2-(benzyloxymethyl)-3,4-bis(benzyloxy)-5-(3,3-dimethoxypropyl)pyrrolidine (**11**).* To a solution of cyclic nitrone **1** (20.0 g, 48.0 mmol) was added dropwise a solution of Grignard reagent in THF (100 mL) [prepared by heating Mg turnings (3.5 g, 144 mmol) and bromide **10** (22 g, 120 mmol) under Barbier conditions]. The reaction mixture was stirred for 30 min, quenched with saturated NH_4Cl (50 mL) solution, and extracted with AcOEt (3 × 100 mL). The combined extracts were dried with $MgSO_4$, and the solvents were removed in vacuo. The residue was recrystallized (petroleum ether/AcOEt 2:1 15 mL) at 0 °C and filtered to give hydroxylamine **11** as a white powder (17.4 g). The filtrate was concentrated and purified by flash column chromatography (silica gel, petroleum ether/AcOEt 3:1) to give hydroxylamine **11** as a white powder (5.6 g): yield 92%; mp 48−50 °C; $[\alpha]_D^{20}$ + 7.6 (c 1.05, CH_2Cl_2); IR (cm^{-1}) 3416, 2931, 1649, 1454, 1122, 738, 698; ^1H NMR (300 MHz, $CDCl_3$) δ 7.33−7.25, (m, 15H), 5.37 (s, 1H, OH), 4.59−4.41 (m, 7H), 3.96−3.94 (m, 1H), 3.81 (dd, J = 2.8, 3.5 Hz, 1H), 3.76−3.75 (m, 1H), 3.59−3.53 (m, 2H), 3.29 (s, 3H), 3.27 (s, 3H), 3.19−3.12 (m, 1H), 1.74−1.59 (m, 4H); ^{13}C NMR (75 MHz, $CDCl_3$) δ 138.2, 138.2, 138.1, 128.4, 128.3, 128.0, 127.9, 127.7, 127.7, 127.6, 104.4, 86.7, 84.7, 73.3, 71.8, 71.6, 70.2, 69.6, 68.4, 52.9, 52.4, 29.5, 23.8; HRMS (ESI) m/z calcd for $[C_{31}H_{39}NO_6H^+]$ 522.2850, found 522.2847 (−0.43 ppm).

*(3S,4S,5S)-2-(Benzyloxymethyl)-3,4-bis(benzyloxy)-5-(3,3-dimethoxypropyl)pyrroline N-Oxide (**12**) and (3S,4S,5S)-2-(3,3-Dimethoxypropyl)-3,4-bis(benzyloxy)-5-(benzyloxymethyl)pyrroline N-Oxide (**13**).* Following the standard deprotection procedure, reaction of activated manganese dioxide (2.78 g, 32 mmol) and hydroxylamine **11** (8.3 g, 16 mmol) gave **12** as a brown oil (3.6 g, 43%) and **13** also as a brown oil (3.2 g, 39%). **12**: $[\alpha]_D^{20}$ +40.0 (c 0.65, CH_2Cl_2); IR (cm^{-1}) 3062, 3031, 2933, 2865, 1717, 1587, 1496, 1360, 1242, 1206, 1069, 1028, 739, 698; ^1H NMR (300 MHz, $CDCl_3$) δ 7.38−7.24 (m, 15H, PhH), 4.69−4.56 (m, 6H, H-6, H-3, 4 × CH_2Ph), 4.24 (s, 2H, 2 × CH_2Ph), 4.38−4.33 (m, 2H, H-6, H-9), 3.95 (d, J = 3.3 Hz, 1H, H-5), 3.83 (s, 1H, H-4), 3.30 (s, 3H, OCH_3), 3.28 (s, 3H, OCH_3), 2.16−2.07 (m, 1H, H-7), 1.88−1.71 (m, 1H, H-7), 1.70−1.59 (m, 2H, H-8); ^{13}C NMR (75 MHz, $CDCl_3$) δ 142.4 (C-2), 137.5, 137.0, 128.5, 128.51, 128.45, 128.10, 128.06, 128.03, 127.99, 127.9, 127.7, 104.2 (C-9), 82.6 (C-3), 80.8 (C-4), 78.8 (C-5), 73.6, 72.5, 71.3, 62.7 (C-6), 53.2, 53.0 (OCH_3), 28.5 (C-8), 26.3 (C-7); HRMS (ESI) m/z calcd for $[C_{31}H_{37}NO_6Na^+]$ 542.2513, found 542.2513. **13**: $[\alpha]_D^{20}$ +26.8 (c 0.82, CH_2Cl_2); IR (cm^{-1}) 3062, 3031, 2933, 2866, 1715, 1599, 1496, 1453, 1362, 1250, 1206, 1122, 1071, 1028, 738, 698; ^1H NMR (300 MHz, $CDCl_3$) δ 7.25−7.16 (m, 15H, PhH), 4.59−4.35 (m, 7H, 6 × CH_2Ph, H-3), 4.27 (t, J = 5.7 Hz, 1H, H-9), 4.15 (t, J = 2.1 Hz, 1H, H-4), 3.97 (s, 1H, H-2), 3.95 (dd, J = 5.4, 9.9 Hz, 1H, H-6), 3.75 (dd, J = 2.7, 9.9 Hz, 1H, H-6), 3.20 (s, 6H, OCH_3), 2.59−2.52 (m, 1H, H-7), 2.42−2.35 (m, 1H, H-7), 1.87−1.73 (m, 2H, H-8); ^{13}C NMR (75 MHz, $CDCl_3$) δ 146.4 (C-2), 137.8, 137.3, 137.2, 128.6, 128.5, 128.4, 128.1, 128.04, 127.97, 127.9, 127.8, 104.1 (C-9), 84.9 (C-3), 78.3 (C-4), 77.4 (C-5), 73.5, 71.7, 71.6, 66.9 (C-6), 53.2, 53.1 (OCH_3), 27.4 (C-8), 20.6 (C-7); HRMS (ESI) m/z calcd for $[C_{31}H_{37}NO_6H^+]$ 520.2694, found 520.2696.

*(3S,4S,5S)-2-(Benzyloxymethyl)-3,4-bis(benzyloxy)-5-(3-oxopropyl)-1-pyrroline N-Oxide (**14**).* To a well-stirred solution of nitrone **12** (0.68 g, 1.31 mmol) in acetone/H_2O (50 mL, 4:1) was added catalytic p-TsOH (25 mg, 0.13 mmol). The reaction mixture was stirred for 2 h at reflux. The acetone was removed in vacuo. The aqueous layer was extracted with ethyl acetate (3 × 10 mL). The combined the organic layers were dried and filtered, and solvents were removed under reduced pressure. The residue was purified by flash column chromatography (silica gel, petroleum ether/AcOEt 1/2) to afford the aldehyde **14** (437 mg, 79%) as a colorless oil: $[\alpha]_D^{20}$ +42.0 (c 1.19, CH_2Cl_2); IR (cm^{-1}) 3062, 3031, 2925, 2864, 2727, 1723, 1588, 1496, 1389, 1358, 1247, 1208, 1093, 1071, 1028, 905, 818, 740, 699 cm^{-1}; ^1H NMR (300 MHz, $CDCl_3$) δ 9.62 (s, 1H, H-9), 7.23−7.17 (m, 15H, PhH), 4.62−4.42 (m, 6H, H-3, H-6, 4 × CH_2Ph), 4.36−4.25 (m, 3H, H-6, 2 × CH_2Ph), 3.89 (t, J = 5.7 Hz, 1H, H-5), 3.71 (s, 1H, H-4), 2.54 (t, J = 7.2 Hz, 2H, H-8), 2.16−2.05 (m, 2H, H-7); ^{13}C NMR (75 MHz, $CDCl_3$) δ 200.6 (C-9), 143.0 (C-2), 137.4, 137.3, 136.9, 128.63, 128.58, 128.5, 128.21, 128.18, 128.1, 128.0, 127.8, 82.5 (C-3), 81.0 (C-4), 77.8 (C-5), 73.6, 72.7, 71.5, 62.7 (C-6), 39.6 (C-8), 23.6 (C-7); HRMS (ESI) m/z calcd for $[C_{29}H_{31}NO_5H^+]$ 474.2275, found 474.2262.

*(1R,2R,5S,6S,7S)-1-(Benzyloxymethyl)-6,7-bis(benzyloxy)-8-azabicyclo[3.2.1]octane-2,8-diol (**15**).* To a stirred and carefully deoxygenated solution of aldehyde **14** (437 mg 0.92 mmol) in THF (18 mL) was added deoxygenated water (1.32 mL, 73.6 mmol) under an Ar atmosphere. The mixture was cooled to −78 °C to which was added freshly prepared SmI_2 in THF (23 mL, 1.84 mmol). The reaction was completed within 10 min and then quenched by successively adding aqueous solutions of $Na_2S_2O_3$ (10 mL) and $NaHCO_3$ (10 mL); the aqueous layer was extracted with ethyl acetate (3 × 10 mL), and the combined organic layers were washed with a saturated aqueous solution of NaCl, dried over $MgSO_4$. Filtration, concentration in vacuo, and purification by chromatography (silica gel, petroleum ether/AcOEt = 4/1) afforded the *N*-hydroxylamino alcohol **15** (284 mg, 65%) as a light yellow oil. **15**: $[\alpha]_D^{20}$ +2.04 (c 0.98, CH_2Cl_2); IR (cm^{-1}) 3505, 3330, 3062, 3030, 2934, 2865, 1495, 1453, 1417, 1362, 1306, 1207, 1188, 1075, 1013, 908, 845, 738, 698 cm^{-1}; ^1H NMR (300 MHz, $CDCl_3$) δ 7.34−7.18 (m, 15H, PhH), 4.62−4.35 (m, 6H), 4.26−3.96 (m, 3H), 3.80−3.69 (m, 2H), 3.62−3.53 (m, 1H), 2.50−2.39 (m, 0.62H), 2.21−2.16 (m, 0.35H), 2.07−1.93 (m, 0.80H), 1.83−1.70 (m, 1.26H), 1.60−1.49 (m, 0.73H), 1.10−1.03 (m, 0.61H); ^{13}C NMR (75 MHz, $CDCl_3$) δ 138.2, 138.1, 138.0, 137.8, 137.4, 128.5, 128.3, 128.3, 128.1, 127.9, 127.8, 127.7, 127.64, 127.56, 127.5, 90.1, 88.3, 83.9, 82.6, 75.1, 73.9, 73.6, 73.1, 72.4, 71.8, 71.3, 71.1, 69.8, 69.2, 68.9, 67.4, 64.5, 26.7, 26.4, 25.3, 16.5; HRMS (ESI) m/z calcd for $[C_{29}H_{33}NO_5H^+]$ 476.2431, found 476.2445.

*(1R,2R,5S,6S,7S)-1-(Benzyloxymethyl)-6,7-bis(benzyloxy)-8-azabicyclo[3.2.1]octane-2-ol (**16**).* Following the standard deprotection procedure, **16** was obtained as a yellow oil (34 mg, 89%): $[\alpha]_D^{20}$ −16.0 (c 1.0, MeOH); IR (cm^{-1}) 3363, 2935, 1128, 1074, 1048, 1011, 898, 773; ^1H NMR (300 MHz, D_2O) δ 4.05 (d, J = 2.4 Hz, 1H, H-7), 4.00 (s, 1H, H-6), 3.80 (s, 1H, H-2), 3.59−3.60 (m, 2H, H-8), 3.12 (s, 1H, H-5), 1.90−1.82 (m, 2H, H-3, H-4), 1.77−1.58 (m, 2H, H-3, H-4); ^{13}C NMR (75 MHz, D_2O) δ 82.3 (C-6), 81.1 (C-7), 67.7 (C-1), 65.1 (C-2), 62.8 (C-8), 61.2 (C-5), 25.3, 24.3 (C-3, C-4); HRMS (ESI) m/z calcd for $[C_8H_{15}NO_4H^+]$ 190.1074, found 190.1071.

Synthesis of 24. *(3aS,4S,5S,6S)-4,5-Bis(benzyloxy)-6-((benzyloxy)methyl)tetrahydropyrrolo[1,2-b]isoxazol-2(3H)-one (**18**).* 1,2-Dibromoethane (0.45 g, 0.22 mL, 0.0024 mol) was added via a syringe to a suspension of Zn powder (3.51 g, 0.054 mol) in anhydrous THF (24 mL). After being heated to reflux for 10 min, the mixture was cooled to room temperature; TMSCl (0.26 g, 0.31 mL, 0.0024 mol) was added, and the mixture was stirred for 15 min. Ethyl bromoacetate **17** (4.01 g, 0.024 mol) and cyclic nitrone **1** (5.00 g, 0.012 mol) were added successively at such a rate that THF boiled gently. After being stirred for 2 h, the reaction mixture was quenched with 1 N hydrochloric acid (10 mL). The aqueous phase was extracted with ethyl acetate (3 × 10 mL) and dried with $MgSO_4$, and the solvent was concentrated in vacuo. The lactone **18** thus obtained as a colorless oil was used directly without purification to the next step: $[\alpha]_D^{20}$ +80.4 (c 0.92, CH_2Cl_2); IR (cm^{-1}) 3062 (w), 3030 (m), 2920 (m), 2865 (m), 1784 (s), 1494 (m), 1454 (m), 1415 (m), 1365 (m), 1208 (m), 1186 (m), 1154 (m), 1099 (s), 1027 (m), 908 (m); ^1H NMR (600 MHz, $CDCl_3$) δ 7.38−7.26 (m, 15H, PhH), 4.61−4.47 (m, 6H, CH_2Ph), 4.19 (t, J = 3.9 Hz, 1H, H-4), 4.15 (td, J = 5.2, 9.8 Hz, 1H, H-2), 4.09 (t, J = 3.9 Hz, 1H, H-3), 3.81 (q, J = 5.0 Hz, 1H, H-5), 3.67 (dd, J = 5.2, 9.9 Hz, 1H, H-6), 3.60 (dd, J = 6.3, 10.0 Hz, 1H, H-6), 2.94 (dd, J = 9.0, 17.8 Hz, 1H, H-7), 2.80 (dd, J = 6.0, 17.8 Hz, 1H, H-7); ^{13}C NMR (75 MHz, $CDCl_3$) δ 174.7 (C-8), 137.8, 137.4, 137.1, 128.7, 128.53, 128.45, 128.2, 128.0, 127.90, 127.89, 127.8, 87.7 (C-3), 84.0 (C-4), 73.41, 72.42 (C-5), 72.38, 72.3, 68.6 (C-6), 68.0 (C-2), 34.4 (C-7); HRMS (ESI) m/z calcd for $[C_{28}H_{29}NO_5Na^+]$ 482.1938, found 482.1936 (−0.34 ppm).

DOI: 10.1021/acs.joc.5b00342
J. Org. Chem. 2015, 80, 4501−4515

*(2S,3S,4S,5S)-1-Hydroxy-2-(benzyloxymethyl)-3,4-bis(benzyloxy)-5-(2-hydroxyethyl)pyrrolidine (**19**).* $LiAlH_4$ (0.91 g, 0.024 mol) was added slowly to a solution of the lactone **18** in anhydrous THF (50 mL) at 0 °C (ice−water bath). After the addition was completed, the reaction mixture was allowed to warm to room temperature and stirred for an additional 1 h, and ethyl acetate was added to destroy excess $LiAlH_4$, followed by acidification with 1 N HCl. The aqueous phase was extracted with ethyl acetate (3 × 15 mL), and the combined organic layer was dried and concentrated. The crude product was used directly for oxidation. **19**: colorless oil; $[\alpha]_D^{20}$ +2.9 (*c* 0.7, CH_2Cl_2); IR (cm^{-1}) 3369 (m), 3062 (w), 3030 (w), 2923 (m), 2869 (m), 1495 (m), 1453 (s), 1363 (s), 1310 (w), 1263 (m), 1209 (m), 1071 (s), 1027(s); ^1H NMR (300 MHz, $CDCl_3$) δ 7.32−7.24 (m, 15H, PhH), 4.59−4.43 (m, 6H, CH_2Ph), 4.01−3.99 (m, 1H, H-3), 3.95 (dd, *J* = 3.0, 6.3 Hz, 1H, H-4), 3.78−3.69 (m, 3H, 2 × H-8, H-6), 3.61−3.54 (m, 2H, H-6, H-2), 3.33 (t, *J* = 6.6 Hz, 1H, H-5), 2.07−1.98 (m, 1H, H-7), 1.86−1.76 (m, 1H, H-7); ^{13}C NMR (75 MHz, $CDCl_3$) δ138.1, 137.9, 137.7, 128.5, 128.44, 128.40, 128.3, 128.1, 128.0, 127.9, 127.8, 127.7, 87.0 (C-4), 84.5 (C-3), 73.3, 72.1, 71.7, 70.3 (C-2), 69.3 (C-5), 67.9 (C-6), 61.1 (C-8), 32.3 (C-7); HRMS (ESI) *m*/*z* calcd for $[C_{28}H_{33}NO_5H^+]$ 464.2431, found 464.2432 (−0.17 ppm).

*(3S,4S,5S)-2-(2-Hydroxyethyl)-3,4-bis(benzyloxy)-5-(benzyloxymethyl)-1-pyrroline N-Oxide (**20**) and (3S,4S,5S)-2-(Benzyloxymethyl)-3,4-bis(benzyloxy)-5-(2-hydroxyethyl)-1-pyrroline N-Oxide (**21**).* Following the standard deprotection procedure, reaction of activated manganese dioxide (2.08 g, 0.024 mol) and the crude hydroxylamine **19** gave **20** as a yellow oil (1 g, 18% for 3 steps) and **21** also as a yellow oil (3 g, 54% for 3 steps). **20**: $[\alpha]_D^{20}$ +9.5 (*c* 1.05, CH_2Cl_2); IR (cm^{-1}) 3335 (m), 3052 (m), 3032 (m), 2918 (m), 2867 (m), 1601 (m), 1494 (m), 1454 (m), 1362 (m), 1266 (s), 1210 (m), 1075 (s), 1092 (s), 1027 (m); ^1H NMR (300 MHz, $CDCl_3$) δ 7.31−7.22 (m, 15H, PhH), 4.67−4.63 (m, 1H, H-4), 4.60−4.29 (m, 6H, 6 × CH_2Ph), 4.26−4.24 (m, 1H, H-5), 4.08 (m, 1H, H-4), 4.04 (q, *J* = 5.1 Hz, 1H, H-6), 3.89−3.59 (m, 3H, H-6, 2H-8), 2.81−2.65 (m, 1H, H-7); ^{13}C NMR (75 MHz, $CDCl_3$) δ146.4 (C-2), 137.7, 137.1, 137.0, 128.6, 128.5,128.3, 128.04, 128.02, 127.84, 127.80, 85.4 (C-3), 78.2 (C-4), 77.6 (C-5), 73.5, 71.9, 71.8, 66.7 (C-6), 59.2 (C-8), 29.8 (C-7); HRMS (ESI) *m*/*z* calcd for $[C_{28}H_{31}NO_5Na^+]$ 484.2094, found 484.2090 (−0.96 ppm). **21**: $[\alpha]_D^{20}$ +89 (*c* 1.55, CH_2Cl_2); IR (cm^{-1}) 3363 (m), 3062 (m), 3030 (m), 2921 (m), 2865 (m), 1598 (m), 1495 (m), 1453 (m), 1394 (m), 1357 (m), 1232 (m), 1208 (m), 1070 (s), 1027 (m); ^1H NMR (300 MHz, $CDCl_3$) δ 7.35−7.24 (m, 15H, PhH), 4.69−4.56 (m, 6H, H-3, H-6, 4 × CH_2Ph), 4.44−4.34 (m, 3H, H-6, 2 × CH_2Ph), 4.07−4.05 (m, 1H, H-5), 3.86 (s, 1H, H-4), 3.80−3.67 (m, 2H, H-8), 2.18−2.06 (m, 1H, H-7), 2.01−1.95 (m, 1H, H-7); ^{13}C NMR (75 MHz, $CDCl_3$) δ144.9 (C-2), 137.3, 137.2, 136.9, 128.7, 128.6, 128.5, 128.2, 128.11, 128.08, 128.05, 128.0, 82.5 (C-3), 81.9 (C-4), 78.7 (C-5), 73.7, 72.8, 71.6, 62.9 (C-6), 59.9 (C-8), 35.7 (C-7); HRMS (ESI) *m*/*z* calcd for $[C_{28}H_{31}NO_5Na^+]$ 484.2094, found 484.2091 (−0.82 ppm).

*(3S,4S,5S)-2-(Benzyloxymethyl)-3,4-bis(benzyloxy)-5-(2-oxoethyl)-1-pyrroline N-Oxide (**22**).* To a solution of oxalyl dichloride (0.17 mL, 1.43 mmol) in CH_2Cl_2 (10 mL) was added dropwise DMSO (0.14 mL, 2.6 mmol) at −70 °C, and the resulting solution was stirred for 20 min. A solution of alcohol **21** (0.6 g, 1.3 mmol) in CH_2Cl_2 (10 mL) was added dropwise at −70 °C, and the resulting solution was stirred for 1 h. Then triethylamine (0.9 mL, 6.5 mmol) was added, and the resulting solution was stirred at −70 °C for 15 min and at room temperature for another 1 h. The resulting mixture was diluted with CH_2Cl_2 (50 mL) and washed with H_2O (3 × 20 mL). The organic phase was dried ($MgSO_4$) and concentrated under reduced pressure to afford aldehyde **15**, which was used in the next step without isolation.

*(1R,2S,3S,4S,6R)-1-(Benzyloxymethyl)-2,3-bis(benzyloxy)-7-azabicyclo[2.2.1]heptane-6,7-diol (**23**).* To a stirred and carefully deoxygenated solution of nitrone **22** (directly obtained from the last step, 0.56 mmol) in THF (26 mL) was added deoxygenated water (0.81 mL, 0.045 mol) under an Ar atmosphere. The mixture was cooled to −78 °C to which was added freshly prepared SmI_2 in THF (14 mL, 1.12 mmol). The reaction was completed within 10 min and quenched by successively added aqueous solutions of NaS_2SO_3 (5 mL) and $NaHCO_3$ (5 mL), the aqueous layer was extracted with ethyl acetate (3 × 10 mL), and the combined organic layers were washed with saturated aqueous solution of NaCl and dried over $MgSO_4$. Filtration, concentration in vacuo, and purification by chromatography on silica gel afforded the *N*-hydroxyamino alcohol **23** (139 mg, 54% for two steps) as a colorless oil: $[\alpha]_D^{20}$ +21.2 (*c* 1.32, CH_2Cl_2); IR (cm^{-1}) 3541 (m), 3354 (m), 3062 (m), 3031 (m), 2920 (m), 2865 (s), 1496 (m), 1453 (m), 1419 (w), 1362 (m), 1309 (m), 1261 (m), 1208 (m), 1092 (s), 1027 (s); ^1H NMR (600 MHz, $CDCl_3$) δ 7.34−7.23 (m, 15H, PhH), 4.62 (d, *J* = 12.0 Hz, 1H, CH_2Ph), 4.52 (d, *J* = 11.8 Hz, 1H, CH_2Ph), 4.51 (d *J* = 11.8 Hz, 1H, CH_2Ph), 4.47 (dd, *J* = 11.8 Hz, 1H, CH_2Ph), 4.45 (dd, *J* = 11.8 Hz, 1H, CH_2Ph), 4.39 (d, 1H, *J* = 11.9 Hz, CH_2Ph), 4.33−4.30 (m, 1H, H-6), 4.02 (d, *J* = 11.1 Hz, 1H, H-7), 4.00 (s, 1H, H-2), 3.88 (d, *J* = 11.1 Hz, 1H, H-7), 3.85 (d, *J* = 5.6 Hz, 1H, H-4), 3.18 (s, 1H, H-3), 2.67 (d, *J* = 10.6 Hz, 1H, OH), 2.16−2.12 (m, 1H, H-5b), 2.00−1.97 (m, 1H, H-5a); ^{13}C NMR (75 MHz, $CDCl_3$) δ138.2, 138.00, 137.95, 128.4, 128.33, 128.31, 127.8, 127.7, 127.6, 83.1 (C-3), 79.9 (C-2), 75.6 (C-1), 73.5, 72.2, 70.9, 72.1 (C-6), 69.0 (C-4), 64.7 (C-7), 37.7 (C-5); HRMS (ESI) HRMS (ESI) *m*/*z* calcd for $[C_{28}H_{31}NO_5H^+]$ 462.2275, found 462.2275 (0.09 ppm).

*(1R,2S,3S,4S,5R)-1-(Hydroxymethyl)-7-azabicyclo[2.2.1]heptane-2,3,6-triol (**24**).* Copper(II) acetate (1.6 mg, 0.008 mmol) was added to a suspension of Fe powder (4.5 mg, 0.8 mmol) in acetic acid (1 mL), and the mixture was stirred at room temperature for 2 h after which the color turned to brown. A solution of **23** (40 mg, 0.087 mmol) in AcOH (1 mL) was added, and after the reaction mixture was stirred at room temperature for 3 h, acetic acid was removed under reduced pressure. The residue was dissolved in ethyl acetate, and the pH adjusted to 8 by adding aqueous solution of $NaHCO_3$ and filtered with Celite. The filtrate was extracted with ethyl acetate (3 × 2 mL), and the combined organic layers were dried (Na_2SO_4) and concentrated at reduced pressure to afford the amine as a brown oil. 10% Pd/C (10 mg) and concd HCl (2 mL) were added to a solution of thus obtained amine in MeOH (10 mL). After the resulting suspension had been stirred under an atmosphere of H_2 at room temperature for 24 h, the reaction was judged to be complete by TLC. The flask was bubbled with Ar, and the Pd/C was filtered off. After the solution was concentrated in vacuo, the residue was dissolved in MeOH and neutralized with aqueous ammonium solution and concentrated in vacuo. The above procedure was repeated three times to ensure complete neutralization. The residue was purified with an acid resin column (DOWEX 50W × 8, 100−200 mesh), eluting with distilled water (50 mL) and then 1 N NH_4OH (50 mL), affording **24** (14 mg, 92% for two steps) as a yellow oil: $[\alpha]_D^{20}$ −3.1 (*c* 0.65, MeOH); IR (cm^{-1}) 3343, 2939, 1086, 1037; ^1H NMR (300 MHz, D_2O) δ 4.30 (dd, *J* = 2.7, 7.2 Hz, 1H, H-6), 3.87 (m, 3H, H-3, 2 × H-7), 3.59 (d, *J* = 1.5 Hz, 1H, H-2), 3.44 (d, *J* = 4.2 Hz, 1H, H-4), 2.12−2.04 (m, 1H, H-5), 1.63−1.55 (m, 1H, H-5); ^{13}C NMR (75 MHz, D_2O) δ 80.0 (C-2), 78.6 (C-3), 72.9 (C-1), 67.0 (C-6), 62.0 (C-4), 58.2 (C-7), 37.5 (C-5); HRMS (ESI) *m*/*z* calcd for $[C_7H_{13}NO_4H^+]$ 176.0917, found 176.0918.

Preparation of Protein Structures. To compare with the corresponding experimental values for rat isomaltase or sucrase, we wanted to use the rat proteins in docking simulations. However, their structures did not exist in protein data banks. Thus, three-dimensional structures of the rat isomaltase and sucrase were constructed by the homology modeling method, based on human isomaltase (PDB ID: 3LPP;[5] identity: 73%) and human maltase (PDB ID: 2QMJ;[8] identity: 38%), respectively. Next, to relax these predicted 3D-structures, we performed the annealing simulations with a molecular dynamic (MD) method. After that, to consider the structural flexibility around the keyhole of isomaltase and sucrase in our docking calculations, keyhole samplings were performed with MD calculations at 300 K from above annealing structures as initial coordinates. In the 200000 MD steps (Δt = 6 [fs]), the 250 keyhole structures were saved. The keyholes were then selected from the 250 sampled structures by clustering. These homology modeling and molecular dynamics samplings were performed with Prime package and Desmond package in Schrödinger Suite 2008,[51] respectively.

DOI: 10.1021/acs.joc.5b00342
J. Org. Chem. 2015, 80, 4501−4515

Molecular Docking Calculations and Binding Energy Estimation. We have performed the docking simulations of miglitol, α-1-C-butyl-DNJ, and α-1-C-butyl-LAB for each keyhole of isomaltase with Glide in Schrödinger Suite 2008.[52] To consider the ionization states around pH 6.8, corresponding to the experimental conditions, in our docking calculations, we used the Ionizer and Epik.[53] Then, many conformations of each ligand state were prepared with confgen Advanced. The poses generated from docking calculations were ranked by Glide Score, and the top 10 ranked poses were selected for each ligand. These poses were optimized with OPLS2005 force field[54] ($\varepsilon = 4r$), and the interaction energies were calculated. A pose with the lowest value of the interaction energy was selected as the binding conformation for each ligand. After these binding structures had been optimized with GB/SA continuum solvation model, we calculated the binding energies (ΔEs) by the below equation, where E_{comp}, $E_{protein}$, and E_{ligand} are a total energy of protein−ligand complex, protein, and ligand, respectively.

$$\Delta E = E_{comp} - (E_{protein} + E_{ligand})$$

Enzyme Assay. Brush border membranes were prepared from the rat small intestine according to the method of Kessler et al.[55] and were assayed at pH 6.8 for rat intestinal isomaltase using the appropriate disaccharide as substrate. The reaction mixture contained 25 mM maltose and the appropriate amount of enzyme, and the incubations were performed for 10−30 min at 37 °C. The reaction was stopped by heating at 100 °C for 3 min. After centrifugation (600 g; 10 min), 0.05 mL of the resulting reaction mixture was added to 3 mL of the Glucose CII-test Wako. The absorbance at 505 nm was measured to determine the amount of the released D-glucose. Kinetic parameters were determined by the double-reciprocal-plot method of Lineweaver−Burk at increasing concentrations of the appropriate maltose.

■ ASSOCIATED CONTENT

Supporting Information

^{1}H and ^{13}C NMR spectra of obtained compounds. This material is available free of charge via the Internet at http://pubs.acs.org.

■ AUTHOR INFORMATION

Corresponding Authors

*E-mail: kato@med.u-toyama.ac.jp.
*E-mail: yucy@iccas.ac.cn.
*E-mail: hironos@pharm.kitasato-u.ac.jp.

Notes

The authors declare no competing financial interest.

■ ACKNOWLEDGMENTS

This work was supported in part by a Grant-in-Aid for Scientific Research (C) (No: 26460143) (A.K.) from the Japanese Society for the Promotion of Science (JSPS) and the Leverhulme Trust (G.W.J.F.). Financial support from the National Basic Research Program of China (Nos. 2011CB808603, 2012CB822101), the National Natural Science Foundation of China (No. 21272240), the National Science and Technology Major Projects for "Major New Drugs Innovation and Development" (2013ZX09508104), the Development Fund for Collaborative Innovation Center of Glycoscience of Shandong University, and National Engineering Research Center for Carbohydrate Synthesis of Jiangxi Normal University is gratefully acknowledged.

■ REFERENCES

(1) Coutinho, M.; Gerstein, H. C.; Wang, Y.; Yusuf, S. *Diabetes Care* **1999**, *22*, 233−240.
(2) Bonora, E.; Muggeo, M. *Diabetologia* **2001**, *44*, 2107−2114.
(3) Ceriello, A. *Diabetes* **2005**, *54*, 1−7.
(4) Van Beers, E. H.; Buller, H. A.; Grand, R. J.; Einerhand, A. W.; Dekker, J. *Crit. Rev. Biochem. Mol. Biol.* **1995**, *30*, 197−262.
(5) Sim, L.; Willemsma, C.; Mohan, S.; Naim, H. Y.; Pinto, B. M.; Rose, D. R. *J. Biol. Chem.* **2010**, *285*, 17763−17770.
(6) Nichols, B. L.; Eldering, J.; Avery, S.; Hahn, D.; Quaroni, A.; Sterchi, E. *J. Biol. Chem.* **1998**, *273*, 3076−3081.
(7) Nichols, B. L.; Avery, S.; Sen, P.; Swallow, D. M.; Hahn, D.; Sterchi, E. *Proc. Natl. Acad. Sci. U.S.A.* **2003**, *100*, 1432−1437.
(8) Sim, L.; Quezada-Calvillo, R.; Sterchi, E. E.; Nichols, B. L.; Rose, D. R. *J. Mol. Biol.* **2008**, *375*, 782−792.
(9) Rossi, E. J.; Sim, L.; Kuntz, D. A.; Hahn, D.; Johnston, B. D.; Ghavami, A.; Szczepina, M. G.; Kumar, N. S.; Sterchi, E. E.; Nichols, B. L.; Pinto, B. M.; Rose, D. R. *FEBS J.* **2006**, *273*, 2673−2683.
(10) Quezada-Calvillo, R.; Sim, L.; Ao, Z.; Hamaker, B. R.; Quaroni, A.; Brayer, G. D.; Sterchi, E. E.; Robayo-Torres, C. C.; Rose, D. R.; Nichols, B. L. *J. Nutr.* **2008**, *138*, 685−692.
(11) Ren, L.; Cao, X.; Geng, P.; Bai, F.; Bai, G. *Carbohydr. Res.* **2011**, *346*, 2688−2692.
(12) Ren, L.; Qin, X.; Cao, X.; Wang, L.; Bai, F.; Bai, G.; Shen, Y. *Protein Cell* **2011**, *2*, 827−836.
(13) Winchester, B.; Fleet, G. W. J. *Glycobiology* **1992**, *2*, 199−210.
(14) Watson, A. A.; Fleet, G. W. J.; Asano, N.; Molyneux, R. J.; Nash, R. J. *Phytochemistry* **2001**, *56*, 265−295.
(15) Asano, N. *Glycobiology* **2003**, *13*, 93R−104R.
(16) Nash, R. J.; Kato, A.; Yu, C-. Y.; Fleet, G. W. J. *Future Med. Chem.* **2011**, *3*, 1513−1521.
(17) Joubert, P. H.; Bam, W. J.; Manyane, N. *Eur. J. Clin. Pharmacol.* **1986**, *30*, 253−255.
(18) Schnack, C.; Roggla, G.; Luger, A.; Schernthaner, G. *Eur. J. Clin. Pharmacol.* **1986**, *30*, 417−419.
(19) Kennedy, F. P.; Gerich, J. E. *Clin. Pharmacol. Ther.* **1987**, *42*, 455−458.
(20) Wisselaar, H. A.; van Dongen, J. M.; Reuser, A. J. *Clin. Chim. Acta* **1989**, *182*, 41−52.
(21) Misago, M.; Tsukada, J.; Fukuda, M. N.; Eto, S. *Biochem. Biophys. Res. Commun.* **2000**, *269*, 219−225.
(22) Belmatoug, N.; Burlina, A.; Giraldo, P.; Hendriksz, C. J.; Kuter, D. J.; Mengel, E.; Pastores, G. M. *J. Inherit. Metab. Dis.* **2011**, *34*, 991−1001.
(23) Best, D.; Jenkinson, S. F.; Saville, A. W.; Alonzi, D. S.; Wormald, M. R.; Butters, T. D.; Norez, C.; Becq, F.; Blériot, Y.; Adachi, I.; Kato, A.; Fleet, G. W. J. *Tetrahedron Lett.* **2010**, *51*, 4170−4174.
(24) Best, D.; Wang, C.; Weymouth-Wilson, A. C.; Clarkson, R. A.; Wilson, F. X.; Nash, R. J.; Miyauchi, S.; Kato, A.; Fleet, G. W. J. *Tetrahedron: Asymmetry* **2010**, *21*, 311−319.
(25) da Cruz, F. P.; Newberry, S.; Jenkinson, S. F.; Wormald, M. R.; Butters, T. D.; Alonzi, D. S.; Nakagawa, S.; Becq, F.; Nash, R. J.; Kato, A.; Fleet, G. W. J. *Tetrahedron Lett.* **2011**, *52*, 219−223.
(26) Ayers, B. J.; Ngo, N.; Jenkinson, S. F.; Martínez, R. F.; Shimada, Y.; Adachi, I.; Weymouth-Wilson, A. C.; Kato, A.; Fleet, G. W. J. *J. Org. Chem.* **2012**, *77*, 7777−7792.
(27) Kato, A.; Hayashi, E.; Miyauchi, S.; Adachi, I.; Imahori, T.; Natori, Y.; Yoshimura, Y.; Nash, R. J.; Shimaoka, H.; Nakagome, I.; Koseki, J.; Hirono, S.; Takahata, H. *J. Med. Chem.* **2012**, *55*, 10347−10362.
(28) Wiltz, O.; O'Hara, C. J.; Steele, G. D.; Mercurio, A. M. *Surgery* **1990**, *108*, 269−276.
(29) Wiltz, O.; O'Hara, C. J.; Steele, G. D.; Mercurio, A. M. *Gastroenterology* **1991**, *100*, 1266−1278.
(30) Delso, I.; Tejero, T.; Goti, A.; Merino, P. *J. Org. Chem.* **2011**, *76*, 4139−4143.
(31) Chavarot-Kerlidou, M.; Rivard, M.; Chamiot, B.; Hahn, F.; Rose-Munch, F.; Rose, E.; Py, S.; Herson, P. *Eur. J. Org. Chem.* **2010**, *75*, 944−958.
(32) Zhang, Z.-L.; Nakagawa, S.; Kato, A.; Jia, Y.-M.; Yu, C.-Y. *Org. Biomol. Chem.* **2011**, *9*, 7713−7719.
(33) Ducrot, P. H.; Lallemand, J. Y. *Tetrahedron Lett.* **1990**, *31*, 3879−3882.

DOI: 10.1021/acs.joc.5b00342
J. Org. Chem. 2015, 80, 4501−4515

(34) Goldmann, A.; Milat, M. L.; Ducrot, P. H.; Lallemand, J. Y.; Maille, M.; Lepingle, A.; Charpin, I.; Tepfer, D. *Phytochemistry* **1990**, *29*, 2125−2127.
(35) Molyneux, R. J.; Pan, Y. T.; Goldmann, A.; Tepfer, D. A.; Elbein, A. D. *Arch. Biochem. Biophys.* **1993**, *304*, 81−88.
(36) Asano, N.; Kato, A.; Oseki, K.; Kizu, H.; Matsui, K. *Eur. J. Biochem.* **1995**, *229*, 369−376.
(37) Asano, N.; Kato, A.; Miyauchi, M.; Kizu, H.; Tomimori, T.; Matsui, K.; Nash, R. J.; Molyneux, R. J. *Eur. J. Biochem.* **1997**, *248*, 296−303.
(38) Kato, A.; Nakagome, I.; Nakagawa, S.; Koike, Y.; Nash, R. J.; Adachi, I.; Hirono, S. *Bioorg. Med. Chem.* **2014**, *22*, 2435−2441.
(39) Cheng, H. H.; Asano, N.; Ishii, S.; Ichikawa, Y.; Fan, J.-Q. *FEBS J.* **2006**, *273*, 4082−4092.
(40) Rasmussen, T. S.; Jensen, H. H. *Org. Biol. Chem.* **2010**, *8*, 433−441.
(41) Rasmussen, T. S.; Allman, S.; Twigg, G.; Butters, T. D.; Jensen, H. H. *Bioorg. Med. Chem. Lett.* **2011**, *21*, 1519−1522.
(42) Wang, W.-B.; Huang, M.-H; Li, Y.-X.; Rui, P.-X.; Hu, X.-G.; Zhang, W.; Su, J.-K.; Zhang, Z.-L.; Zhu, J.-S.; Xu, W.-H.; Xie, X.-Q.; Jia, Y.-M.; Yu, C.-Y. *Synlett* **2010**, *3*, 488−492.
(43) Yu, C.-Y.; Huang, M.-H. *Org. Lett.* **2006**, *8*, 3021−3024.
(44) Merino, P.; Delso, I.; Tejero, T.; Cardona, F.; Marradi, M.; Faggi, E.; Parmeggiani, C.; Goti, A. *Eur. J. Org. Chem.* **2008**, *73*, 2929−2947.
(45) Hu, X.-G.; Bartholomew, B.; Nash, R. J.; Wilson, F. X.; Fleet, G. W. J.; Nakagawa, S.; Kato, A.; Jia, Y.-M.; Well, R. V.; Yu, C.-Y. *Org. Lett.* **2010**, *12*, 2562−2565.
(46) Hu, X.-G.; Jia, Y.-M.; Xiang, J.; Yu, C.-Y. *Synlett* **2010**, 982−986.
(47) Cicchi, S.; Goti, A.; Brandi, A. *J. Org. Chem.* **1995**, *60*, 4743−4748.
(48) Cicchi, S.; Marradi, M.; Goti, A.; Brandi, A. *Tetrahedron Lett.* **2001**, *42*, 6503−6505.
(49) Masson, G.; Py, S.; Vallée, Y. *Angew. Chem., Int. Ed.* **2002**, *41*, 1772−1775.
(50) Masson, G.; Philouze, C.; Py, S. *Org. Biomol. Chem.* **2005**, *3*, 2067−2069.
(51) Bowers, K. J.; Chow, E.; Xu, H.; Dror, R. O.; Eastwood, M. P.; Gregersen, B. A.; Klepeis, J. L.; Kolossvary, I.; Moraes, M. A.; Sacerdoti, F. D.; Salmon, J. K.; Shan, Y.; Shaw, D. E. *Proc. ACM/IEEE Conf. Supercomputing (SC06)*, Tampa, FL, Nov 11−17, 2006.
(52) Friesner, R. A.; Banks, J. L.; Murphy, R. B.; Halgren, T. A.; Klicic, J. J.; Mainz, D. T.; Repasky, M. P.; Knoll, E. H.; Shelley, M.; Perry, J. K.; Shaw, D. E.; Francis, P.; Shenkin, P. S. *J. Med. Chem.* **2004**, *47*, 1739−1749.
(53) Shelley, J. C.; Cholleti, A.; Frye, L. L.; Greenwood, J. R.; Timlin, M. R.; Uchimaya, M. *J. Comput. Aided Mol. Des.* **2007**, *21*, 681−91.
(54) Jorgensen, W. L.; Maxwell, D. S.; Tirado-R, J. *J. Am. Chem. Soc.* **1996**, *118*, 11225−11236.
(55) Kessler, M.; Acuto, O.; Strelli, C.; Murer, H.; Semenza, G. A. A. *Biochem. Biophys. Acta* **1978**, *506*, 136−154.

DOI: 10.1021/acs.joc.5b00342
J. Org. Chem. 2015, 80, 4501−4515